# SYNTHESIS AND CHARACTERIZATION OF ZSM-35

A THESIS SUBMITTED TO
THE GRADUATE SCHOOL OF NATURAL AND APPLIED SCIENCES
OF
THE MIDDLE EAST TECHNICAL UNIVERSITY

BY

ZUHAL COŞKUN

IN PARTIAL FULFILLMENT OF THE REQUIREMENTS FOR THE DEGREE OF

MASTER OF SCIENCE

IN

THE DEPARTMENT OF CHEMICAL ENGINEERING

JULY 2003

Approval of the Graduate School of Natural and Applied Sciences:

Prof. Dr. Canan Özgen
Director

I certify that this thesis satisfies all the requirements as a thesis for the degree of Master of Science.

Prof. Dr. Timur Doğu
Head of Department

This is to certify that we have read this thesis and that in our opinion it is fully adequate, in scope and quality, as a thesis and for the degree of Master of Science.

Prof. Dr. Ali Çulfaz
Co-Supervisor

Prof. Dr. Hayrettin Yücel
Supervisor

Examining Committee Members

Assoc. Prof. Dr. Gürkan Karakaş

Prof. Dr. Suna Balcı

Asst. Prof. Dr. Halil Kalıpçılar

Prof. Dr. Ali Çulfaz

Prof. Dr. Hayrettin Yücel

# ABSTRACT

## SYNTHESIS AND CHARACTERIZATION OF ZSM-35

Coşkun, Zuhal

M.Sc., Department of Chemical Engineering

Supervisor: Prof. Dr. Hayrettin Yücel

Co-Supervisor: Prof. Dr. Ali Çulfaz

July 2003, 102 pages

ZSM-35, a medium pore size, high silica zeolite of ferrierite structure has been synthesized using hydrothermal methods. ZSM-35 was synthesized from an aqueous gel of composition 1.85 $Na_2O$. $Al_2O_3$. x $SiO_2$. 592 $H_2O$. 19.7 R. The parameters of the syntheses were $SiO_2/Al_2O_3$ ratio ($10 < x < 25$), crystallization temperature (150 °C < T < 225 °C), crystallization time ($0 < t < 480$ h) and the type of organic template (R: pyrrolidine or ethylenediamine).

ZSM-35 was synthesized as pure phase from the experiments which were carried out with the batch composition having $SiO_2/Al_2O_3$ ratio of 20 and 25 at

177 °C, in presence of pyrrolidine. Then, the experiments were performed at $SiO_2/Al_2O_3$ ratio of 20 with pyrrolidine or ethylenediamine at temperatures 150, 177, 200 and 225 °C. At temperatures 150, 177 and 200 °C, ZSM-35 synthesis was achieved as pure phase with both templates. In the experiments performed at 225 °C, ZSM-35 was synthesized with ethylenediamine as the only crystalline phase. In the synthesis carried out with pyrrolidine, there exist a minor mordenite phase along with ZSM-35.

ZSM-35 crystals synthesized with pyrrolidine at 150, 177 and 200 °C were observed to be spherical crystal agglomerates of 15-20 μm size with crystallites smaller than 1 μm. The morphology of the zeolites synthesized with ethylenediamine at temperatures 150, 177, 200 and 225 °C exhibits spherical crystal agglomerates composed of platelet crystallites.

The methanol sorption capacity of ZSM-35 synthesized with pyrrolidine at 25 °C and at the relative pressure $P/P_0 = 0.5$ was 0.1380 $cm^3/g$ corresponding to 88.4 % the total pore volume. In the sorption experiments carried out at 0 °C, sample synthesized with pyrrolidine was measured to sorb methanol with higher capacity than the one synthesized with ethylenediamine. The methanol sorption capacity of ZSM-35 sample synthesized with ethylenediamine at 0 °C and at the relative pressure $P/P_0 = 0.4$ was measured as 0.1363 $cm^3/g$ corresponding to 87.3 % of the total pore volume.

Keywords: ZSM-35, Synthesis, Pyrrolidine, Ethylenediamine, Methanol Sorption.

# ÖZ

# ZSM-35 SENTEZİ VE KARAKTERİZASYONU

Coşkun, Zuhal

Yüksek Lisans, Kimya Mühendisliği Bölümü

Tez Yöneticisi: Prof. Dr. Hayrettin Yücel

Yardımcı Tez Yöneticisi: Prof. Dr. Ali Çulfaz

Temmuz 2003, 102 sayfa

Hidrotermal sentez yöntemleri kullanılarak, orta boyut gözenekli, yüksek silikalı, ferrierit yapısında bir zeolit olan ZSM-35 üretimi gerçekleştirilmiştir. ZSM-35, kompozisyonu 1.85 $Na_2O$. $Al_2O_3$. x $SiO_2$. 592 $H_2O$. 19.7 R olan sulu jelden üretilmiştir. Sentez parametreleri $SiO_2/Al_2O_3$ oranı ($10 < x < 25$), kristalleşme sıcaklığı ($150\ °C < T < 225\ °C$), kristalleşme zamanı ($0 < t < 480$ saat) ve organik şablon çeşitleridir (R: pirolidin ya da etilendiamin).

ZSM-35, başlangıç kompozisyonundaki $SiO_2/Al_2O_3$ oranı 20 ve 25 olan, 177 °C de ve pirolidin kullanılarak yapılan deneylerde saf faz olarak elde edilmiştir. Daha sonra deneyler $SiO_2/Al_2O_3$ oranı 20 alınarak, pirolidin ya da

etilendiamin kullanılarak 150, 177, 200 ve 225 °C de yapılmıştır. ZSM-35 150, 177 ve 200 °C de her iki şablonla da tek faz olarak üretilmiştir. 225 °C de etilendiamin kullanılarak yapılan deneylerde ZSM-35 tek faz olarak elde edilmiştir. Aynı sıcaklıkta pirolidin kullanılarak yapılan deneylerde ZSM-35'in yanında az miktarda mordenit fazı bulunmuştur.

150, 177 ve 200 °C pirolidinle sentezlenen ZSM-35 kristallerinin 15-20 μm büyüklüğünde küresel kristal yığınları şeklinde, büyüklüğü 1 μm den küçük olan kristalitlerden oluştuğu gözlemlenmiştir. Etilendiamin kullanılarak 150, 177, 200 ve 225 °C de sentezlenen zeolitlerin morfolojisi tabaka şeklinde kristalitlerden oluşan küresel kristal yığınları şeklinde kendini göstermektedir.

Pirolidinle üretilen ZSM-35'in metanol sorpsiyon kapasitesi 25 °C de ve relatif basınç $P/P_0$ = 0.5 te gözenek hacminin % 88.4'üne tekabül eden 0.1380 $cm^3/g$ olarak ölçülmüştür. 0 °C de yapılan deneylerde, pirolidinle üretilen örneğin etilendiaminle üretilen örneğe göre daha fazla metanol sorpsiyon kapasitesine sahip olduğu ölçülmüştür. Etilendiaminle üretilen ZSM-35 örneğinin metanol sorpsiyon kapasitesi 0 °C ve relatif basınç $P/P_0$ = 0.4 te gözenek hacminin % 87.3'üne tekabül eden 0.1363 $cm^3/g$ olarak ölçülmüştür.

Anahtar Kelimeler: ZSM-35, Sentez, Pirolidin, Etilendiamin, Metanol Sorpsiyonu.

*To My Parents*

*Nazife & Mehmet Coşkun*

*and*

*To My Grandmother*

*The Late Münevver Dirlik*

# ACKNOWLEDGEMENTS

I wish to express my deepest gratitude to my supervisors, Prof. Dr. Hayrettin Yücel and Prof. Dr. Ali Çulfaz for their outstanding guidance and encouragement throughout this study.

I am very grateful for the techinal assistance provided by Kerime Güney and Mihrican Açıkgöz for the chemical and thermogravimetric analyses. I also would like to thank Cengiz Tan from Metallurgical Engineering Department of METU for arranging electron microscopy.

I wish to thank my family for their great support, encouragement and unshakable faith in me.

Finally, my special thanks go to Yusuf Göğebakan, for his understanding, endless patience and encouragement on me.

# TABLE OF CONTENTS

# LIST OF TABLES

# LIST OF FIGURES

# CHAPTER 1

# INTRODUCTION

## 1.1. Introduction to Zeolites and ZSM-35

Zeolites are microporous, crystalline, hydrated alumina silicates with a framework structure. Their three-dimensional, polyanionic networks are constructed of $SiO_4$ and $AlO_4$ tetrahedra linked through shared oxygen atoms. The tetrahedral units join together in order to form several ring and cage structures. Depending on the structure type, they contain regular channels or interlinked voids whose aperture diameters are in micropore range. These pores contain water molecules and the cations necessary to balance the negative charge of the framework.

Zeolites may naturally occur or they can be synthesized. More than 150 zeolite types have been synthesized and 40 zeolite types are known to occur in nature as minerals.

Zeolite synthesis can be defined as a kind of art. The crucial step in synthesis process is the preparation of the synthesis mixture (gel). The feasibility and ability to tune the gel composition according to the product requirements

makes this step so important. This means that the synthesis process is easy to handle but any variation in process parameters changes the product properties and even the product. The factors affecting the zeolite synthesis can be ordered as the composition of the synthesis mixture (e.g. $SiO_2/Al_2O_3$ ratio in gel composition constraints the framework of zeolite and as this ratio increases thermal stability, hyrophobicity of the zeolites increase), the homogeneity of the synthesis mixture, the nature of the reactants, initial and final pH of the system, crystallization temperature and the template molecules. There are many facilities of using templating agents such as balancing the framework charge, governing the zeolite morphology and pore size, also affecting phase purity and product yield.

Zeolites are microporous materials with uniform pore dimensions that certain molecules may enter these pores while others are rejected. This property leads to selective adsorption processes. For that reason, they are referred as *molecular sieves.*

Ferrierites are considered as one of the most siliceous zeolites. They can be found in nature as mineral or they can be synthesized artificially. Mineral ferrierite occur in cavities of volcanic rocks or in sedimentary deposits at Si/Al ratio between 4 and 7. Ferrierites can be synthesized at higher Si/Al ratios in single phase form. Several synthetic zeolites were patented as distinct zeolite phases all having a framework structure closely related to the ferrierite type. Fu-9 (Seddon and Whittam, 1985), Nu-23 (Whittam, 1986), ISI-6 (Morimoto *et al.*, 1984) and ZSM-35 (Plank *et al.*, 1977) have ferrierite framework topology.

ZSM-35 is a high silica zeolite having ferrierite structure. Its synthesis can be carried out hydrothermally in an aqueous or a nonaqueous medium with or

without the presence of templating agents. Because of its high Si/Al ratio, it remains thermally stable even at high temperatures. Its unique pore structure is highly selective that it is mostly used in sorption processes. It is a good candidate to be used as a shape selective catalyst in chemical processes like hydrocarbon conversion, isomerization, aromatization and cracking.

## 1.2 Scope of the Study

The aim of this study is synthesizing ZSM-35 in pure phase and investigating the limits of crystallization of ZSM-35 by changing synthesis parameters. The products are to be further characterized in terms of crystallinities, morphologies, thermal behavior and adsorption properties.

The synthesis of ZSM-35 is to be carried out with hydrothermal methods under autogeneous pressure. The products are to be characterized by XRD, SEM, EDAX and TGA methods. Thermal stabilities of the products are to be determined from heat treatment experiments. Also, the sorption capacities of ZSM-35 samples are to be measured for methanol in a gravimetric sorption apparatus at 0 °C and 25 °C.

# CHAPTER 2

# LITERATURE SURVEY

## 2.1 Ferrierite Structure and Synthesis

The zeolite ferrierite is known both as a mineral as well as a synthetic material. Mineral ferrierite was firstly discovered by Graham (1918) near Kamloops Lake in British Columbia, Canada. It was firstly believed as a rare mineral until its abundant occurrence was reported in the studies of the period 1965 to 1971. The formula of the natural ferrierite is given as $(Na,K)_4$. $Mg_2(Si_{30}Al_6)O_{72}$. $(OH)_{20}$. 18 $H_2O$. Ferrierite was firstly synthesized unknowingly by Coombs *et al.* (1959). It was synthesized hydrothermally from a lime-soda-alumina-silicate system at 330 °C in association with mordenite. (Kibby *et al.*, 1974).

### 2.1.1 Crystal Structure of Ferrierite

The crystal structure of ferrierite was determined by Vaughan (1966) and by Kerr (1967). The structure consists of two mutually perpendicular channels formed by ten and eight membered rings (MRs). The aluminosilicate lattice of

ferrierite contains parallel channels formed by 10 membered rings (MRs) having major and minor axes of size 5.5 and 4.3 Å respectively. They are intersected with parallel channels formed by 8 MRs of size 4.8 x 3.4 Å. Ferrierite crystals differ morphologically from other zeolites in having a layer structure. The FER framework topology is shown in Figure 2.1 and the channel system of ferrierite is schematically shown in Figure 2.2.

### 2.1.2 Synthesis Studies

After the initial synthesis by Coombs (1959), Barrer and Marshall (1965) synthesized a strontium zeolite, Sr-D. X-ray powder diffraction pattern of their product was closely related to that of natural ferrierite. The synthesis was carried out from an aqueous gel composition of (1-1.2) SrO. $Al_2O_3$. (7-9) $SiO_2$ at 340-380 °C. Cormier and Sand (1967) synthesized Na and K forms of ferrierite hydrothermally from alumina-silica gel at temperatures of 230- 310 °C.

Kibby *et al.* (1974) synthesized sodium and sodium-tetramethylammonium ferrierites under hydrothermal conditions at 300- 325 °C. They produced pure phase Na- ferrierite using sodium aluminate and colloidal silica sol from a batch composition of $Na_2O$. $Al_2O_3$. 12 $SiO_2$. 250 $H_2O$ both in the presence or absence of tetramethylammonium hydroxide solution.

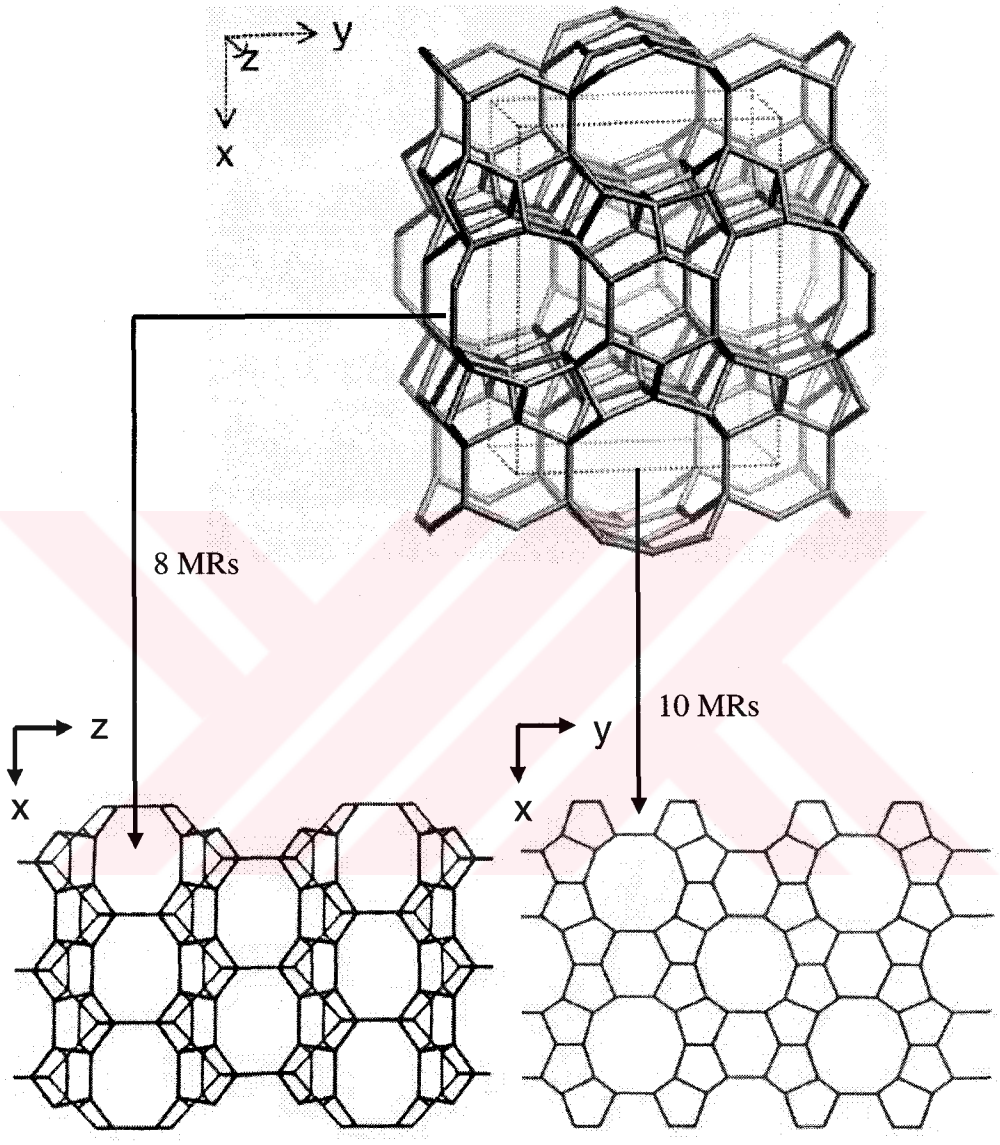


*Figure 2.1 Three Dimensional Ferrrierite Framework Having 10 Membered Rings (MRs) in x-y Direction and 8 Membered Rings (MRs) in x-z Direction (Tütüncü, 2003)*

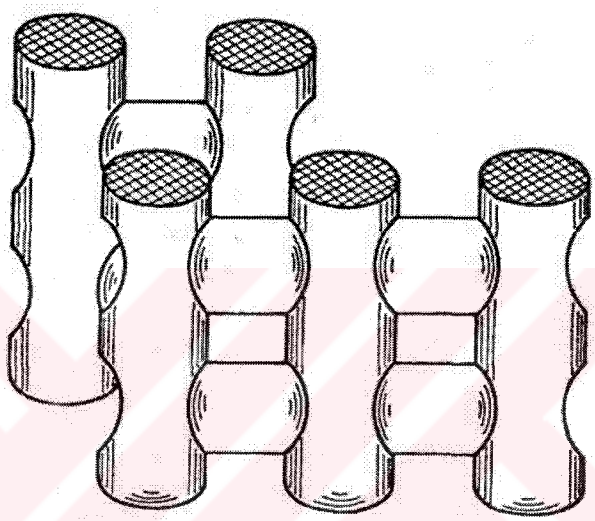

*Figure 2.2 Schematic Representation of Channel System of Ferrierite (Jacobs and Martens, 1987)*

ZSM-35 which is a high silica zeolite with ferrierite topology was firstly synthesized by Plank *et al.* (1977) in a system containing organic template ethylenediamine or pyrrolidine. The gel composition of ZSM-35 in the anhydrous state was expressed in terms of mole ratios of oxides as (0.3-2.5) $R_2O$. (0-0.8) $Na_2O$. $Al_2O_3$. >8 $SiO_2$. R represents the organic nitrogen-containing cation.

ZSM-35 synthesis can be achieved in the presence or absence of organic templates. Araya and Lowe (1985) have investigated the synthesis of novel zeolites from a template free system composed of $K_2O$. $Al_2O_3$. $SiO_2$. $NH_2(CH_2)_6NH_2$. The nature of final product was primarily determined by the $SiO_2/Al_2O_3$ ratio of reactant gel. ZSM-5 was obtained using reactant gels with $SiO_2/Al_2O_3$ ratios of 60:1 whereas ferrierite formation was favored with reactant gels having $SiO_2/Al_2O_3$ ratios of 30:1. Phases containing both ferrierite and ZSM-5 were obtained from reactant gels with $SiO_2/Al_2O_3$ between these two values.

In the study of Çulfaz and Yılmaz (1985), the same system is used as in Cormier and Sand (1967). Ferrierite was synthesized from an aqueous template free gel having molar composition of 1.6 $Na_2O$. 1.6 $K_2O$. $Al_2O_3$. 13.5 $SiO_2$. 130 $H_2O$. 0.8 $CO_2$. 2.4 $(HCO_2)_2$ at 250 °C.

In most of the studies organic templating agents were used in the synthesis mixtures. Fjellvag *et al.* (1989), synthesized ferrierite from Na-TMA (tetra methyl ammonium) containing gel. X-ray diffraction analysis showed that the basic framework for natural and synthetic ferrierite is to be similar but some distinctions occur with respect to non-framework atoms. This study also compared the structural and thermal properties of Na-TMA (calcined)- Ferrierite, H- Ferrierite

and natural ferrierite. H- Ferrierite structure was obtained to be stable up to 952 °C.

In the study of Valyocsik *et al.* (1985) the crystallization of high silica zeolites in the presence of α, ω-diamines at pH< 12 were investigated. The molar composition of the gel for obtaining pure ferrierite formation was 4.2 $C_{3-4}DN$. 0.09 $Na_2O$. $Al_2O_3$. 30 $SiO_2$. 7.8 $H_2O$. The experiments were performed in 300 $cm^3$ stainless steel autoclaves at 170 °C with stirring at 200 rpm. It is found that the ferrierite structure forms most readily from reaction mixtures having $SiO_2$/ $Al_2O_3$ ratio of 12 to 60, whereas MFI structure forms readily even in the absence of alumina. As the carbon amount in diamine functional group increases in gel composition, the zeolite framework changes from FER ( 8 and 10 MRs, both are straight and perpendicular) to a MFI (10 MRs, one straight, other sinusoidal and perpendicular) and to a MEL (10 MRs, both are straight and perpendicular) structural type. A correlation between the dimensions of the respective diamines and the sorption properties of the synthesized zeolites is given. Also, it is proposed that protonated amines exert a templating effect on crystallization.

Gies and Gunawardane (1987) have synthesized aluminum-free form of ferrierite using ethylenenediamine and boric acid as templates in aqueous medium. Almost 100 % yield of aluminum-free ferrierite was obtained at 180 °C in 8 weeks. The product was obtained to be stable up to 1000 °C. Over that temperature the product was turned out to cristobalite.

Workdone by Forbes *et al.* (1995), showed the importance of $SiO_2/Al_2O_3$ ratio in synthesis. They have synthesized Theta-1, ZSM-5, and ferrierite and mordenite type of zeolites together with a dense phase of cristobalite from

aqueous gels containing potassium / sodium hydroxide / chloride, diethanolamine as structure-directing agent at different $SiO_2/Al_2O_3$ ratios. $OH^-/SiO_2$ ratio for ferrierite synthesis was reported to be in the range of 0.075 to 0.105 and $SiO_2/Al_2O_3$ ratio was between 10 and 30. The phase boundaries were found to be generally discrete with the exception of the boundary between ferrierite and ZSM-5. On increasing the $SiO_2/Al_2O_3$ ratio approximately from 16 to 25 (at $OH/SiO_2$ ratio of 0.13), the product altered gradually from ferrierite to ZSM-5 via a continuous series of mixed phases.

In the study of Borade and Clearfield (1994), batch composition of $Na_2O$. $Al_2O_3$. 20 $SiO_2$. 8 R. 448.5 $H_2O$ was used for synthesizing ZSM-35 where R represents the structure-directing agent trimethylcetylammonium hydroxide (TMCAH). ZSM-35 was obtained at 160 °C and 144 h with mordenite as a minor phase. The crystal structure of ZSM-35 synthesized by using TMCAH is stable up to 1000 °C.

Robson (1998) synthesized ZSM-35 from an aqueous gel composition of 1.85 $Na_2O$. $Al_2O_3$. 15.2 $SiO_2$. 592 $H_2O$. 19.7 R system. R represents the organic template ethylenediamine. The crystallization temperature was 177 °C and the crystallization of the product was completed in 10 days. The product was reported as ferrierite (FER), the crystalline phase, and competing phases were quartz, MOR and MFI. From the elemental analysis of the products, $SiO_2/Al_2O_3$ ratio was obtained as 13.

Long *et al.* (2000) studied synthesis, structural characterization and adsorption properties of K, Na-FER synthesized from the system composed of ($6.55K_2O$+$4.21Na_2O$). $Al_2O_3$. 13.5 $SiO_2$. 6.5 $HCO_3$. 116 $H_2O$. Sodium silicate,

silica sol and fumed silica were tested as silica sources, and sodium aluminum sulfate, aluminum hydroxide and meta kaolin were tested as alumina sources. Pure K, Na-FER was obtained at 208 °C from the gel prepared with sodium silicate and sodium aluminum sulfate. It was stated that the starting materials, gel composition and crystallization temperature affects products in great manner. The product structure was totally collapsed and transformed to cristobalite at 1019 °C.

ZSM-35 can also be synthesized in non-aqueous reaction medium. For instance, ZSM-35 was synthesized by Wenyang *et al.* (1989) from non-aqueous system composed of (20-45) Ethylenediamine (ED). (1-8) $Na_2O$. (15-50) $SiO_2$. $Al_2O_3$. (40-420) $(C_2H_5)_3N$. The synthesis was carried out at temperatures from 150 to 200 °C for 96 hours. It was shown that the position and intensity of ZSM-35 peaks synthesized from non-aqueous and aqueous systems are identical. In non aqueous system instead of water triethylamine is used in batch composition. The crystallization mechanisms of non-aqueous and aqueous systems were completely different since ZSM-35 crystallizes from an aqueous system by a liquid transformation and it crystallizes from a non-aqueous system by a solid transformation. The crystallization of ZSM-35 from non-aqueous system is strongly depending on the molar percent of triethylamine and $SiO_2$ and the molar ratio of $Na_2O$/triethylamine. The advantages of non-aqueous synthesis include higher product yields, better control of the molar ratio of $SiO_2$ to $Al_2O_3$ in the products.

Also in the study of Kanno *et al.* (1994) ferrierite, ZSM-48 and ZSM-5 were synthesized from a non-aqueous system where glycerol was used as the solvent and the products encapsulated glycerol molecules in their framework. The

crystallization temperature was 210 °C. The crystallization fields of these three zeolites were obtained. Ferrierite and ZSM-48 retained their zeolitic structure up to 1000 °C whereas ZSM-5 structure was destroyed at 950 °C. The optimum starting gel composition for synthesizing ferrierite was estimated as (3- 15) $Na_2O$. $Al_2O_3$. (12- 48) $SiO_2$. (57- 213) Glycerol.

### 2.1.3 Sorption Studies

The regular nature of the pores and their apertures, whose dimensions are of the same order of magnitude as molecular diameters, enables the zeolites to function as molecular sieves. This is the outstanding property of zeolites that gives them their value as selective adsorbents for separating substances and as shape-selective catalysts. Depending on the zeolite type and its pore system, molecules can penetrate into the cavity system or be excluded from it.

Figure 2.3 shows some of the sorbate zeolites and the possible sorbents. Methanol and ZSM-35 are also added to the original figure.

As it is seen from Figure 2.3, ZSM-35 pore structure is able to sorb many molecules such as $NH_3$, $H_2O$, $H_2$, $CO_2$, $O_2$, $N_2$, methanol, n-butane and ethanol. There are many studies on sorption measurements of ferrierites for many sorbates including methanol. Methanol is known to fill both 8 and 10 membered rings of ZSM-35. Its high packing density within the pores of ZSM-35 and rapid equilibrium in the order of several minutes makes it a suitable probe molecule for ZSM-35 characterization.

In the study of Harrison *et al.* (1987) the shape selective properties of ferrierite, ZSM-5 and ZSM-11 were compared and the effect of mixed zeolitic

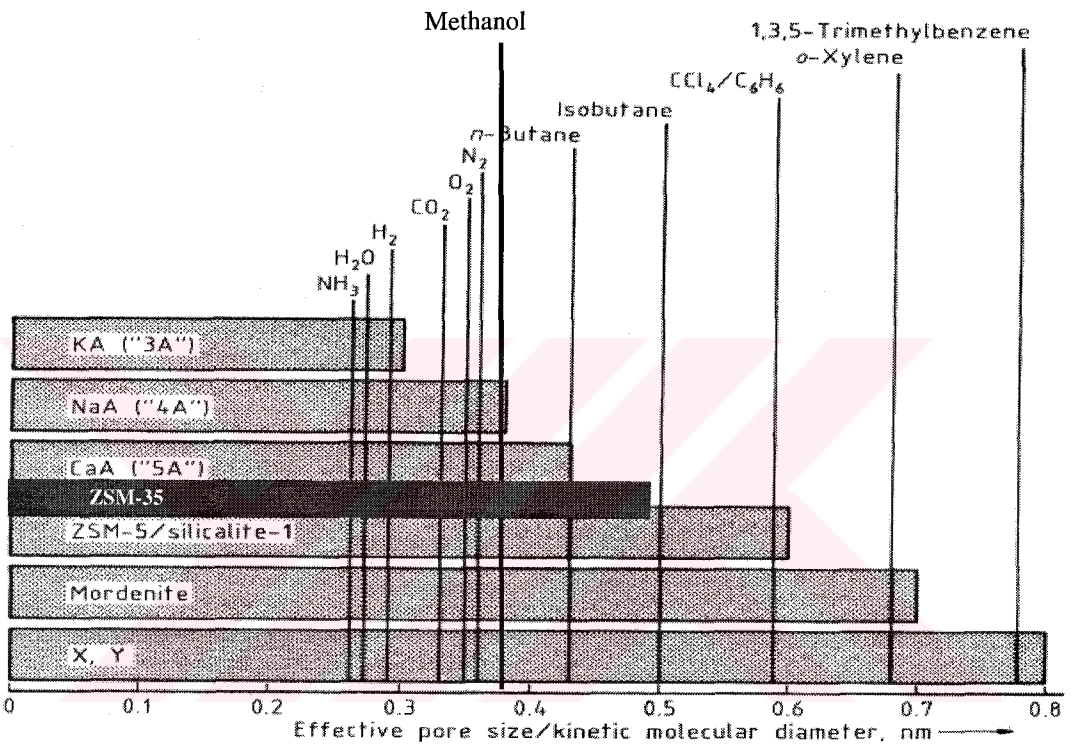


*Figure 2.3 Correlations between the Effective Pore Size of Industrially Important Zeolites and the Kinetic Molecular Diameter of Selected Compounds at Room Temperature (Elvers and Hawkins, 1996)*

phases on the catalysts were investigated. Characterization of the pore structures was performed by measuring the rates and extents of adsorption of molecules with different kinetic diameter. The sorption data of ferrierite revealed that water and methanol are more rapidly adsorbed than n-pentane, n-hexane, benzene, p-xylene, o-xylene and cyclohexane. This arose in part from the decreased hydrophobicity of ferrierite relative to ZSM-5 and ZSM-11, moreover from the ability of the water and methanol molecules to diffuse into both 8 and 10 MRs of ferrierite. The methanol sorption capacity of pure phase ferrierite products were reported to be 86.9 % of the total pore volume.

Kıvanç (1992) studied on the sorption measurements of synthetic and natural ferrierites for water, ethanol, methanol, hexane and toluene molecules at 25 °C. Ferrierites were synthesized from a Na, K containing gel (Çulfaz and Yılmaz, 1985). The sorption measurements were investigated on H-ferrierites. Synthetic ferrierite observed to have higher sorption capacities. Methanol and water molecules were sorbed with the highest capacity. 50.7 % of the total pore volume was measured to fill with methanol. Ethanol and toluene sorbents were totally excluded from 8 MR channels.

Karslı *et al.* (2003) also searched the sorption properties of synthetic ferrierite used in the study of Kıvanç (1992). They determined the limiting sorption volumes of H-ferrierite for sorbates; water, methanol, propane, hexane and ortho-meta-para-xylenes. They obtained isotherms for mentioned liquid vapors and gases at 25°C and at a relative pressure of $P/P_0$=0.5 by using a gravimetric sorption apparatus. Methanol which has a kinetic diameter significantly smaller than the pore dimensions was sorbed relatively rapidly and

filled 77 % of the total pore volume of the zeolite. It is reported that hexane is able to fill only 10 MR channels whereas propane is able to fill both 10 and 8 MR channels and among the xylene isomers, para-xylene having the smallest kinetic diameter of three isomers is sorbed to a greater extent than the others.

Öztin (1997) studied on the sorption capacities and rates of Na and H forms of ZSM-35. Measurements were performed at room temperature for water, methanol, hexane, benzene, o/m/p-xylene and ethylbenzene. ZSM-35 samples sorbed methanol and water with the highest capacity. 73.7 % of the total pore volume was reported to be filled with methanol.

Long *et al.* (2000) studied the sorption of nitrogen, n-hexane and methanol and on K, Na-ferrierite at room temperature. Comparing the pore size with the sorbent molecule size, they estimated that nitrogen was adsorbed by both 10 and 8 MRs whereas n-hexane and methanol were adsorbed by only 10 MRs. The sorption volume of methanol was observed to be lower than that of n-hexane at $P/P_0 < 0.05$. On the other hand methanol sorption is evidently greater than n-hexane on the samples at low partial pressure. The filling of methanol was given as 54.5 % at $P/P_0 = 0.6$. It was also stated that the micropore volume and loading of methanol increase with the removal of $K^+$ and $Na^+$ cations from the structure.

Tütüncü (2003) worked on the sorption of Na and H ZSM-35 for methanol and ethanol. Na form of ZSM-35 showed higher sorption capacity than H form. Also, the sorption capacity of ZSM-35 for ethanol was observed to be higher than that for methanol. 73.7 % of the total pore volume was filled with methanol at $P/P_0 = 0.5$.

# CHAPTER 3

# EXPERIMENTAL

## 3.1 Synthesis of ZSM-35

This partial study on crystallization field of ZSM-35 was carried out for the purpose of synthesizing pure and highly crystalline products from an aqueous gel composition of 1.85 $Na_2O$. $Al_2O_3$. x $SiO_2$. 592 $H_2O$. 19.7 R, where $10 < x < 25$ and R is pyrrolidine (Py) or ethylenediamine (ED). The temperature range of crystallization was from 150 to 225 °C and the crystallization period was in the range of 0 to 480 hours. The basis of these conditions was described by Robson (1998) as a procedure. The synthesis conditions for that particular batch were x = 15.2, T = 177 °C and t = 240 hours and the template was ethylenediamine.

All the experiments performed in this study are shown in Table 3.1 in detailed form, with the batch codes, molar batch compositions and crystallization temperatures.

*Table 3.1 Molar Batch Compositions and Crystallization Temperatures Used in ZSM-35 Synthesis*

| Batch Code | Part No | Molar Batch Composition | T ( °C) |
|---|---|---|---|
| Z3 | 1 | 1.85 $Na_2O$. $Al_2O_3$. 15.2 $SiO_2$. 592 $H_2O$. 19.7 Py | 177 |
| Z5 | 1-2 | 1.85 $Na_2O$. $Al_2O_3$. 20 $SiO_2$. 592 $H_2O$. 19.7 Py | 177 |
| Z8 | 1 | 1.85 $Na_2O$. $Al_2O_3$. 25 $SiO_2$. 592 $H_2O$. 19.7 Py | 177 |
| Z9 | 1 | 1.85 $Na_2O$. $Al_2O_3$. 10 $SiO_2$. 592 $H_2O$. 19.7 Py | 177 |
| Z11 | 2 | 1.85 $Na_2O$. $Al_2O_3$. 20 $SiO_2$. 592 $H_2O$. 19.7 Py | 225 |
| Z12 | 2 | 1.85 $Na_2O$. $Al_2O_3$. 20 $SiO_2$. 592 $H_2O$. 19.7 Py | 200 |
| Z13 | 2 | 1.85 $Na_2O$. $Al_2O_3$. 20 $SiO_2$. 592 $H_2O$. 19.7 Py | 150 |
| Z14 | 3 | 1.85 $Na_2O$. $Al_2O_3$. 20 $SiO_2$. 592 $H_2O$. 19.7 ED | 200 |
| Z15 | 3 | 1.85 $Na_2O$. $Al_2O_3$. 20 $SiO_2$. 592 $H_2O$.19.7 ED | 225 |
| Z16 | 3 | 1.85 $Na_2O$. $Al_2O_3$. 20 $SiO_2$. 592 $H_2O$. 19.7 ED | 177 |
| Z17 | 3 | 1.85 $Na_2O$. $Al_2O_3$. 20 $SiO_2$. 592 $H_2O$. 19.7 ED | 150 |

## 3.2 Batch Preparation

The raw materials used in the synthesis were colloidal silica (LUDOX AS-30, 30 wt. % $SiO_2$, Aldrich, lot no: 02302DO), sodium hydroxide (pure pellets, Merck, lot no: B102362 802), aluminum hydroxide (pure powder, Merck, lot no: K24826491 817), pyrrolidine (99 %, Aldrich, lot no: S05094-061) and ethylenediamine (99.5 %, Aldrich, lot no: 01746DI-081).

The synthesis gel was prepared by mixing sodium aluminate solution (Solution A) with the mixture composed of colloidal silica and template (Solution B) which were prepared separately. Solution A was prepared by adding aluminum hydroxide powder on sodium hydroxide solution. This mixture was heated on hot plate and stirred for about 1 h in order to dissolve alumina particles. After a clear sodium aluminate solution was obtained, the evaporated amount of water was added to the solution. Solution B was prepared by adding the template on colloidal silica. This solution was also stirred by magnetic stirrer. Next, solution B was put on to solution A and the mixture was stirred further for about half an hour at room temperature. Gelation occurred immediately upon mixing. At this stage, the reaction mixture had a molar composition of 1.85 $Na_2O$. $Al_2O_3$. x $SiO_2$. 592 $H_2O$. 19.7 R. The gel was poured into stainless steel autoclaves with PTFE inserts of 30-35 ml capacity (Figure 3.1). The autoclaves were then heated in an oven at temperatures ranging from 150 to 225 °C. To stop the crystallization process, the autoclaves were removed from the oven and quenched with cold water. The resultant solid product was recovered by washing with distilled water and filtering until the pH was 8. Finally, the products were dried at 100 °C overnight and kept over saturated potassium sulfate solution placed in a desiccator vessel. Both the

gel that was poured into the autoclaves and the dry product were weighed. Flowchart of the synthesis process is shown in Figure 3.2.

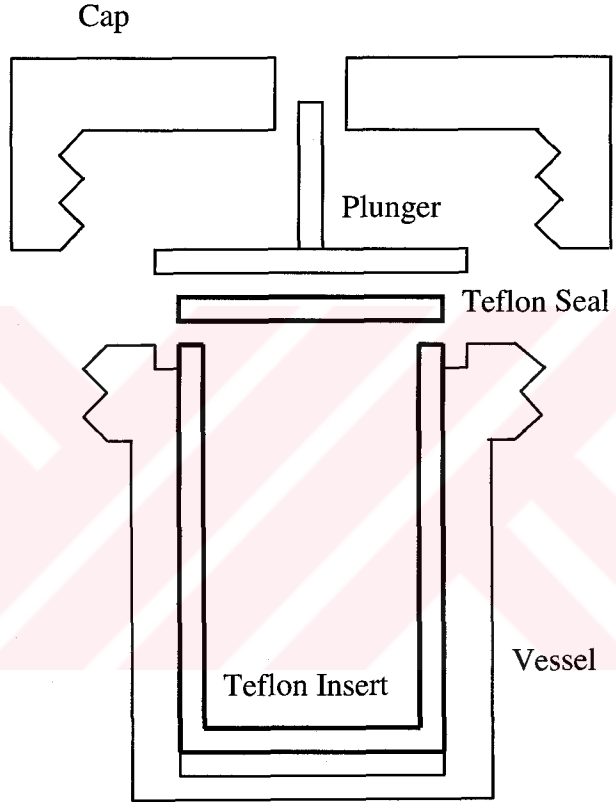


*Figure 3.1 Front View of the Autoclave Used in Syntheses.*

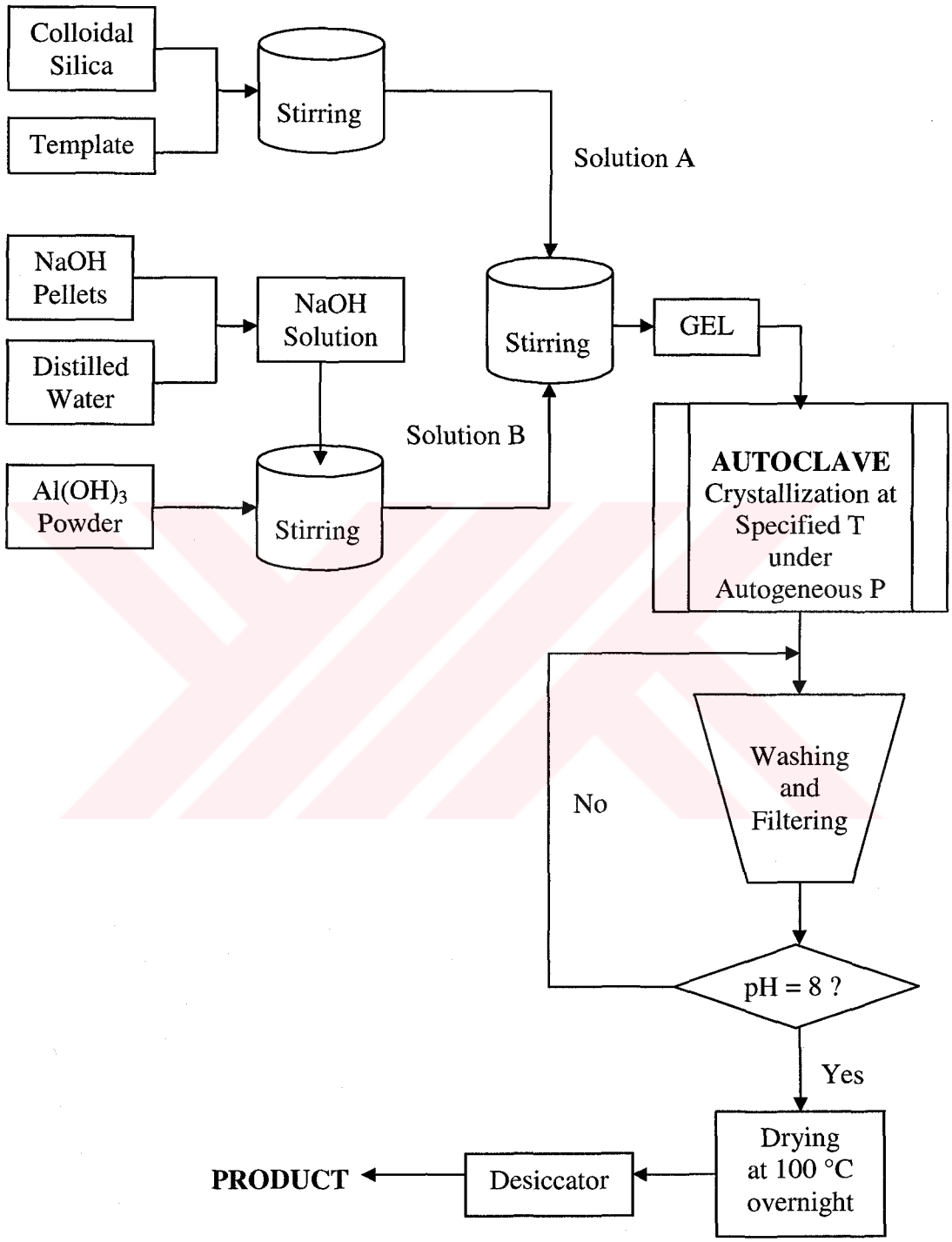


*Figure 3.2 Flowchart of Synthesis Procedure*

## 3.3 Characterization by X-Ray Diffraction (XRD)

The products were identified qualitatively from their X-ray diffraction patterns taken by a Phillips PW1840 diffractometer using CuKα radiation. The samples were placed either in depression mounts or smear mounts depending on the quantity available for scanning. The scanning conditions are given in Table 3.2

*Table 3.2 XRD Scanning Conditions*

| | |
|---|---|
| Anode | Cu |
| Filter | Ni |
| Radiation | CuKα (1.5405 Å) |
| Tube Potential | 30 kV |
| Tube Current | 24 mA |
| Step Size | 0.01 ° |
| Angle (2 Theta) | 5-40 ° |
| Scan Speed | 0.1 ° /s |
| Intensity Range | 10000 counts/s |
| Time Constant | 1 s |
| Slit | 0.2 mm |

In order to quantify the crystallinity of the products, a reference pattern was selected. Crystallinity index of samples were calculated by intensity summation method. For this calculation in the X-ray diffraction pattern, 20 intense peaks that form the characteristics of ZSM-35 structure were selected. These peaks are described in Table 3.3 on a sample ZSM-35 pattern data given by Szostak (1992). The crystallinity index was calculated by Equation 3.1.

$$\text{Crystallinity Index} = \frac{\sum_{n=1}^{20} I_{n,s}}{\sum_{n=1}^{20} I_{n,0}} \qquad (3.1)$$

In the equation, $I_{n,s}$ represents the peak intensity data of the synthesized sample and $I_{n,0}$ represents the peak intensity data of the reference sample. Reference sample peak intensity data was formed by averaging the intensity summations of 20 peaks of the most crystalline ZSM-35 samples. The reference pattern is described in detail in Appendix A1.

% Yield of the syntheses processes were calculated from the weights of gels forming the batch and the products.

The yield of particular run was calculated from Equation 3.2.

$$\%\ \text{Yield} = \frac{\text{Weight of Product (g)}}{\text{Weight of Batch (g)}} \times 100 \qquad (3.2)$$

$SiO_2$/ $Al_2O_3$ ratio of the products were obtained from EDAX (Energy Dispersive X-Ray Analysis) results. Maximum yield can be defined as the maximum amount of zeolite that can be synthesized from a certain molar batch composition. For the calculation of maximum yield for each batch $SiO_2$/ $Al_2O_3$ ratio in zeolite structure should be known. In our case, $SiO_2$/ $Al_2O_3$ ratios in the structure were taken as 20 for the batches having $SiO_2/Al_2O_3$ ratio of 20 and 25, 13 for the batches having $SiO_2/Al_2O_3$ ratio of 15.2 and 10 for the batch having $SiO_2/Al_2O_3$ ratio of 10. Sample calculation for maximum yield is given in Appendix A3.

The percent conversions based on the limiting reactant were calculated by Equation 3.3.

$$\% \text{ Conversion} = \frac{\text{Yield}}{\text{Maximum Yield}} \times \text{Crystallinity Index} \qquad (3.3)$$

*Table 3.3 d-Spacing, Bragg Angle and Relative Intensity Data for 20 Major peaks of Sample XRD Pattern of ZSM-35 (Szostak, 1992)*

| Peak No | d-Spacing | Bragg Angle 2 (Theta) | $I/I_0$ |
|---|---|---|---|
| | 11.48 | 7.70 | 5 |
| 1 | 9.53 | 9.28 | 27 |
| 2 | 7.07 | 12.52 | 25 |
| | 6.93 | 12.77 | 25 |
| 3 | 6.61 | 13.39 | 27 |
| 4 | 5.76 | 15.38 | 12 |
| | 5.67 | 15.63 | 4 |
| | 5.25 | 16.89 | 4 |
| 5 | 4.95 | 17.92 | 10 |
| | 4.58 | 19.38 | 4 |
| 6 | 3.98 | 22.34 | 63 |
| 7 | 3.93 | 22.62 | 39 |
| 8 | 3.85 | 23.10 | 20 |
| 9 | 3.77 | 23.60 | 51 |
| | 3.73 | 23.86 | 12 |
| 10 | 3.66 | 24.32 | 33 |
| 11 | 3.53 | 25.23 | 100 |
| 12 | 3.47 | 25.67 | 80 |
| 13 | 3.39 | 26.29 | 28 |
| 14 | 3.31 | 26.94 | 24 |
| 15 | 3.13 | 28.52 | 18 |
| 16 | 3.04 | 29.38 | 8 |
| 17 | 2.95 | 30.26 | 6 |
| 18 | 2.91 | 30.65 | 2 |
| | 2.84 | 31.41 | 3 |
| | 2.70 | 33.15 | 3 |
| 19 | 2.63 | 33.98 | 7 |
| | 2.60 | 34.40 | 3 |
| | 2.57 | 34.87 | 4 |
| | 2.53 | 35.35 | 2 |
| 20 | 2.47 | 36.33 | 4 |
| | 2.44 | 36.77 | 2 |

## 3.4 Characterization by Scanning Electron Microscope (SEM)

The morphologies and crystal sizes of the synthesized samples were observed by Leo 435VP (Variable Pressure Scanning) Zeiss-Leica Scanning Electron Microscope in Turkish Cement Manufacturers Association. The initial observations were also done by optical microscopy. The micrographs of SEM were taken in the magnification range of 1,000 to 10,000 times. During the SEM study, EDAX (Energy Dispersive X-Ray Analysis) method was applied in order to get a semi- quantitative data of the Si/Al atomic ratio of the synthesized samples. EDAX analyses of the products were performed by JSM-6400 Electron Microscope (JEOL) in Metallurgical Engineering Department of METU.

## 3.5 Characterization by Thermo Gravimetric Analysis (TGA)

The hydration behavior of ZSM-35 was investigated by Thermo Gravimetric Analysis (TGA) which was performed with Du Pont 2000 thermal gravimetric analyzer under nitrogen or air flow between temperatures of 30- 900 °C. The heating rate of the process was 5 or 10 °C/min. From TGA data the removal temperature of templates pyrrolidine and ethylenediamine, water contents of the products were determined.

## 3.6 Thermal Stability Test

Thermal stability test was applied in order to obtain the structure breakdown temperature of the synthesized ZSM-35 samples. For this purpose, about 0.6 g of samples was placed in crucibles. This was the minimum amount needed for smear mount scan of XRD. Then, they were exposed to a heat treatment in the oven for 0.5, 1 and 2 hours. Samples were treated at different temperatures in the range of 200 to 1100 °C. The heating rate was 20 °C/min. Up to 1000 °C treatments, the samples were putting in the oven after it has reached the treatment temperature and then they left in the oven for the desired lengths of time. But, for higher temperatures the crucibles were placed in oven at the beginning of the heating process. After the treatment the crucibles were taken from the oven and kept in dry desiccator until analysis. The changes in the structure of the treated products were observed by XRD analysis and the changes in XRD patterns were investigated.

## 3.7 Sorption Capacity Measurements

Sorption capacities of some high crystallinity ZSM-35 samples for sorbate methanol at 0 °C and 25 °C were measured in a conventional gravimetric adsorption system which was used in the study of Öztin (1997). This system was consisted of an electronic balance enclosed in a vacuum chamber, a high-vacuum pump unit, doser chambers and valves. The pressures were recorded by a pressure transducer and electronic manometer. The sorbate was loaded with the aid of doser chambers containing methanol (Fluka). 30-40 mg of the sample was placed

in an aluminum sample pan and in order to remove water from zeolite structure, it was treated at 673 K under vacuum of less than $10^{-2}$ Pa for about 4 h. Then, the sample was cooled to 0 or 25 °C in a thermostat and methanol was given to the system. The schematic diagram of sorption apparatus is shown in Figure 3.4.

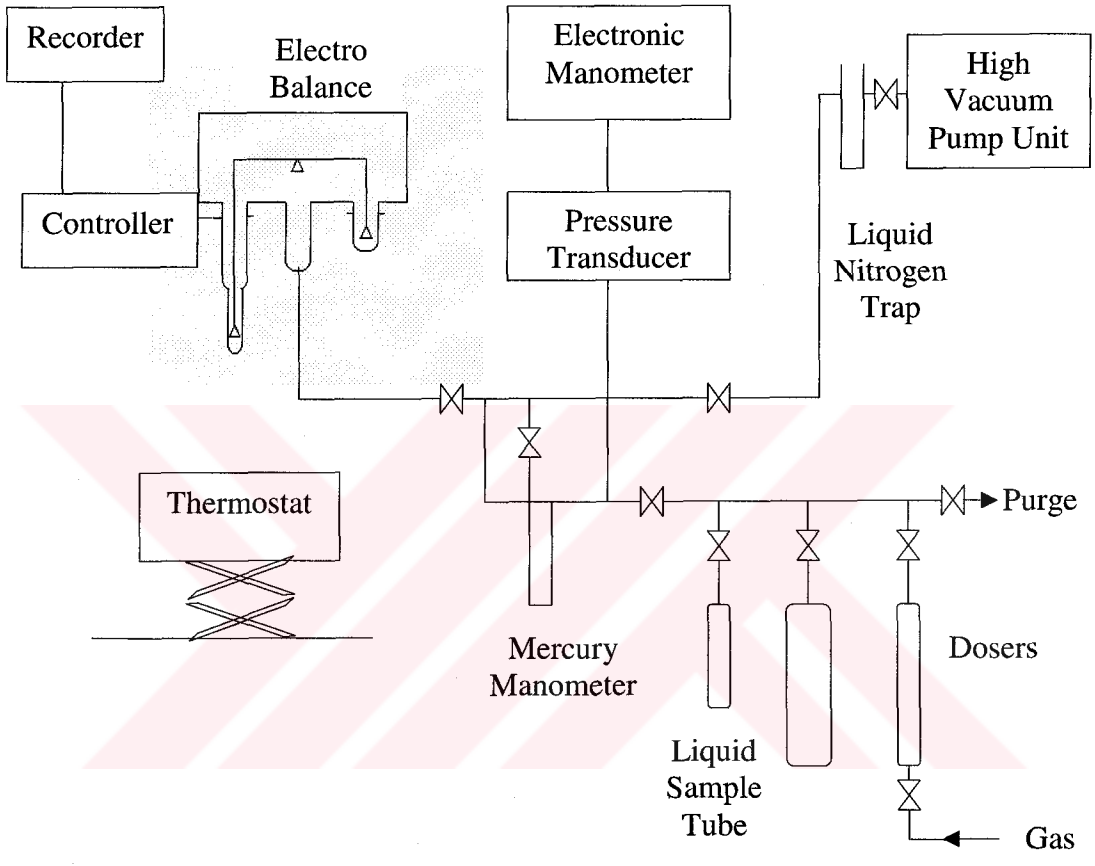


*Figure 3.3 Schematic Diagram of Gravimetric Sorption Apparatus (Öztin, 1997)*

# CHAPTER 4

# RESULTS AND DISCUSSIONS

## 4.1 Synthesis of ZSM-35

In this study synthesis and characterization of ZSM-35 was carried out. ZSM-35 was synthesized from a sodium and pyrrolidine (Py) or ethylenediamine (ED) containing gel with molar composition of 1.85 $Na_2O$. $Al_2O_3$. x $SiO_2$. 592 $H_2O$. 19.7 R under hydrothermal conditions and autogeneous pressure. For synthesizing pure ZSM-35 and also investigating the limits of crystallization of ZSM-35, process parameters were changed in the system. The parameters of the synthesis processes were $SiO_2/Al_2O_3$ ratio, crystallization temperature, crystallization time and type of the organic template (R).

The X-ray diffraction data for a sample ZSM-35 (ZC42) synthesized in this study is compared with the published X-ray diffraction data for several natural and synthetic ferrierites in the form of a line chart indicating the diffraction intensity in Figure 4.1. Peak listing of the samples are given in Appendix C.

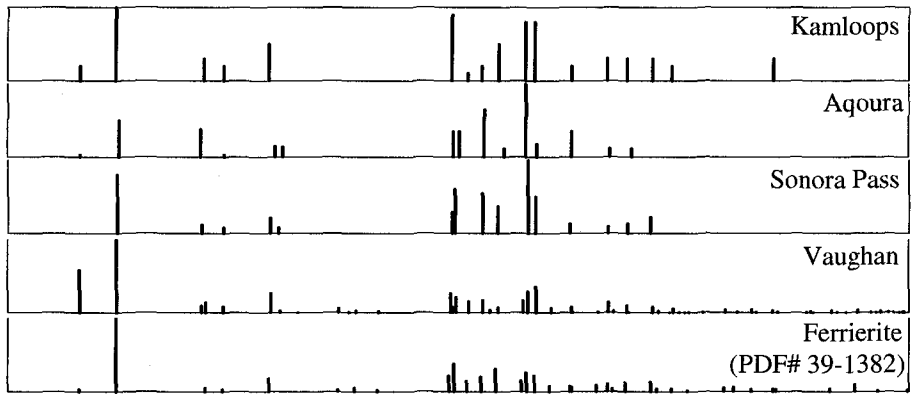


(a)

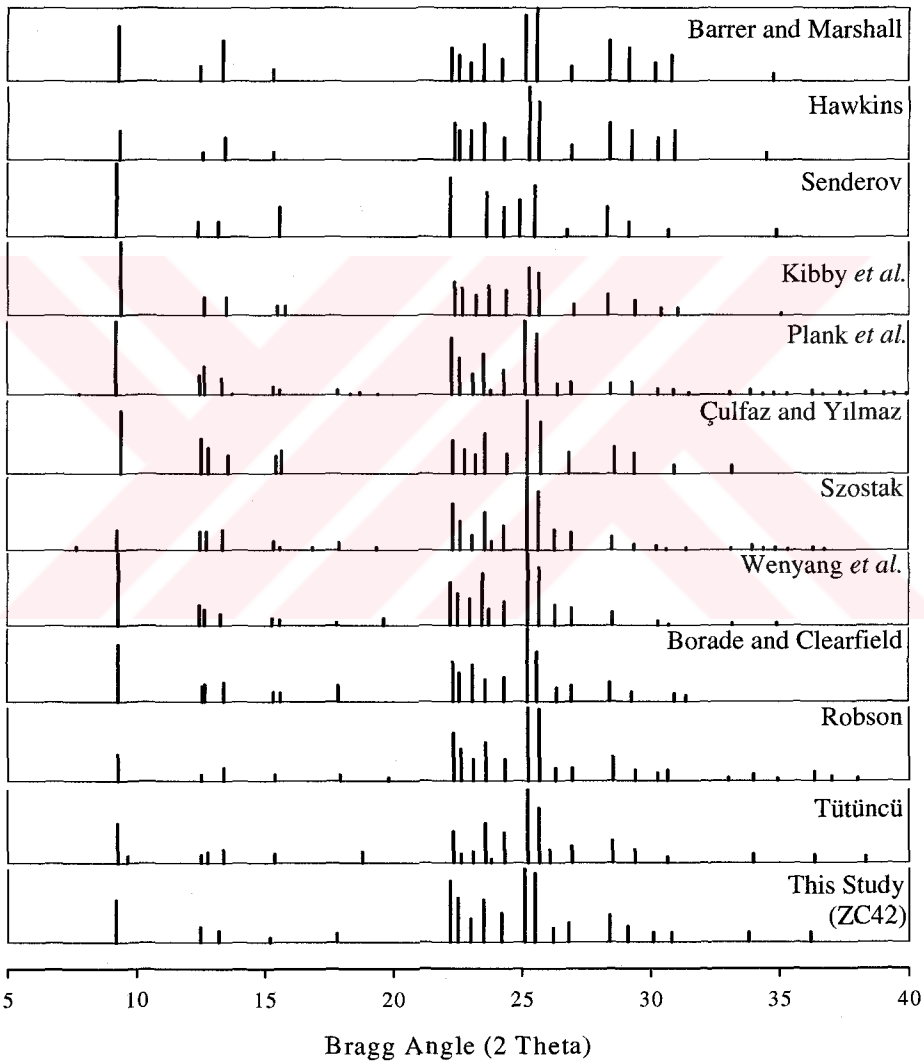


(b)

*Figure 4.1 X- Ray Diffraction Data of (a) Natural (b) Synthetic Ferrierites*

All the peaks of the synthesized sample are consistent with the published X-ray diffraction data of synthetic ferrierites. The peak at d-spacing 11.3 has seen mostly in natural ferrierites.

## 4.2 Crystallization Results

The experiments were carried out mainly in three groups. In the first group named as Part 1, $SiO_2/Al_2O_3$ ratio was changed in the range of 10 to 25 for achieving pure phase synthesis. Another aim of investigation in this group of experiments was to determine the limits of $SiO_2/Al_2O_3$ ratio for synthesizing of pure phase product ZSM-35 at 177 °C in the presence of template pyrrolidine. The limits of this ratio to be attempted in Part 1 were planned by considering the previous studies on ferrierite synthesis under similar experimental conditions. For instance, Forbes *et al.* (1995) offer a $SiO_2/Al_2O_3$ ratio range for ferrierite synthesis between 10 and 20 and noticed that as this range was increased the products were turn out to be different zeolites. Araya and Lowe (1985) proposed the ratio of 30. Also Jacobs and Martens (1987) noted this range between 15 and 35. The crystallization field of ferrierites was estimated between $SiO_2/Al_2O_3$ ratio of 12 and 48 by Kanno *et al.* (1994). In the starting molar batch composition this ratio was given as 15.2 (Robson, 1998).

In the other groups namely Part 2 and Part 3, the $SiO_2/Al_2O_3$ ratio of the batch composition was fixed at 20 and the behavior of crystallization with respect to temperature and time was investigated in the presence of two common organic templates for synthesizing ZSM-35, pyrrolidine (Part 2) and ethylenediamine

(Part 3). Temperature range for ferrierite synthesis was given from 180 to 250 °C in the studies of Gies and Gunawardane (1987) and Long *et al.*, (2000). Syntheses were accomplished in this study at temperatures 150, 177, 200 and 225°C.

### 4.2.1 Crystallization Results of the Experiments Performed at Different $SiO_2/Al_2O_3$ Ratios

Table 4.1 shows the results that were calculated for the first group of experiments that were performed at $SiO_2/Al_2O_3$ ratio of 20. In Table 4.2 and Table 4.3 the crystallinity results for the second and third groups that were performed at $SiO_2/Al_2O_3$ ratio of 25 and 15.2 were also given. The results table for the last group ($SiO_2/Al_2O_3$ ratio 10) was submitted in Table A3. The experimental conditions for syntheses were also submitted in the table headings.

Figure 4.2 gives the sample XRD pattern of pure phase synthesized ZSM-35 pattern at the $SiO_2/Al_2O_3$ ratio of 25 (ZC55). Figure 4.3 shows the XRD patterns of the products synthesized at different time periods within the same batch composition having $SiO_2/Al_2O_3$ ratio of 20. Figure 4.4 shows the effect of $SiO_2/Al_2O_3$ ratio on crystallization of ZSM-35.

The crystallinity and percent conversion data tabulated in Table 4.3 was calculated by considering only the pure peaks of ZSM-35 in XRD patterns. The sample calculation of such cases was shown in Appendix A1.

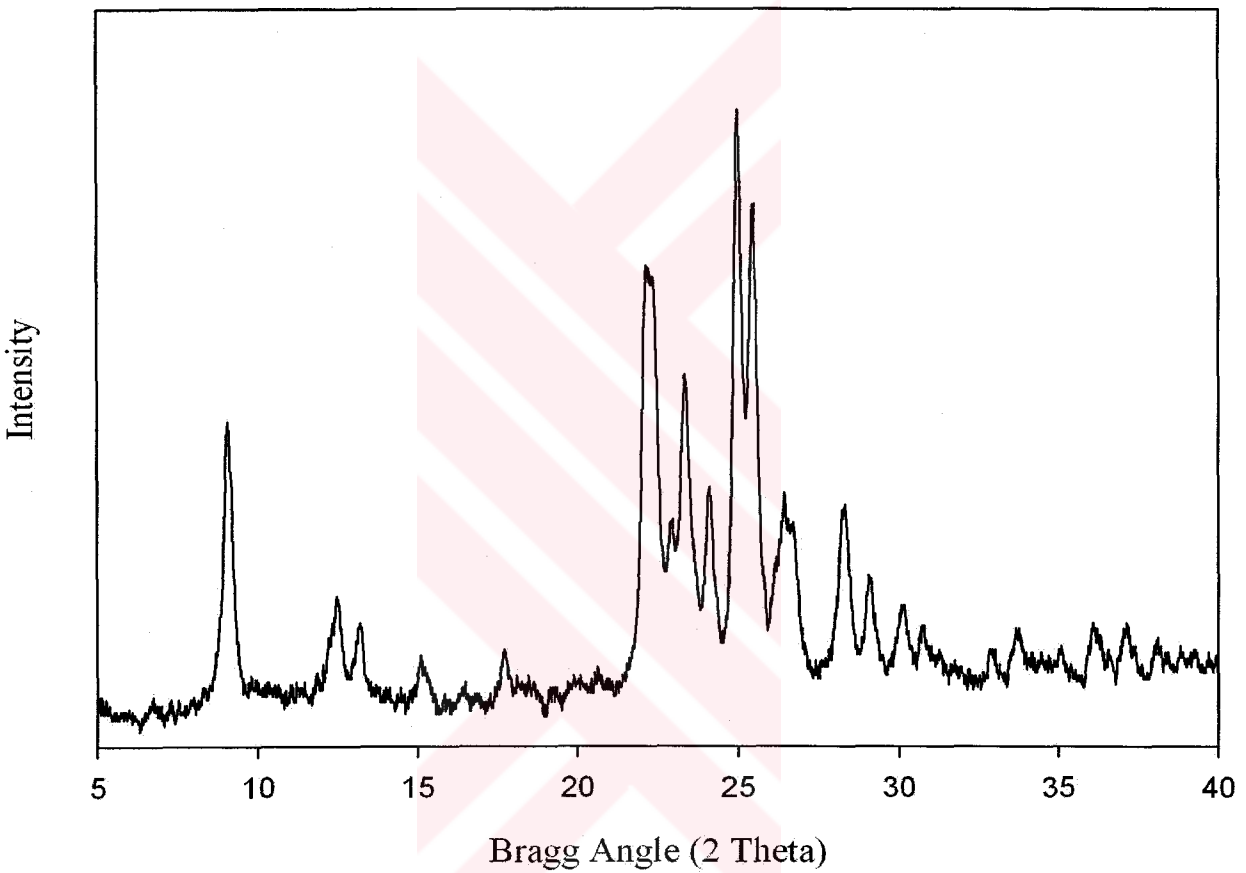


*Figure 4.2 XRD Pattern of ZSM-35 Sample Synthesized from a Molar Batch Composition of 1.85 $Na_2O$. $Al_2O_3$. 25 $SiO_2$. 592 $H_2O$. 19.7 Py at 177 °C for 120 h.*

*Table 4.1 Crystallization of ZSM-35 from a Molar Batch Composition of 1.85 $Na_2O$. $Al_2O_3$. 20 $SiO_2$. 592 $H_2O$. 19.7 Py at T = 177 °C*

| Batch Code | Sample Code | Crystallization Time (h) | Crystalline Phases | Weight of Batch (g) | Weight of Product (g) | % Yield | Crystallinity Index | Yield/ Maximum Yield | % Conversion |
|---|---|---|---|---|---|---|---|---|---|
| Z5 | ZC93 | 0 | Amorphous | - | - | - | - | - | - |
| | ZC39 | 15 | Amorphous | - | - | - | - | - | - |
| | ZC94 | 18 | ZSM-35 Amorphous | - | - | - | - | - | - |
| | ZC95 | 24 | ZSM-35 Amorphous | 31.85 | 2.92 | 9.17 | 0.38 | 0.78 | 29.6 |
| | ZC96 | 36 | ZSM-35 Amorphous | 28.53 | 2.40 | 8.41 | 0.33 | 0.71 | 23.4 |
| | ZC97 | 48 | ZSM-35 Amorphous | 31.62 | 2.84 | 8.98 | 0.47 | 0.75 | 35.2 |
| | ZC41 | 72 | ZSM-35 | 34.05 | 2.78 | 8.16 | 0.90 | 0.69 | 62.1 |
| | ZC42 | 192 | ZSM-35 | 37.57 | 3.58 | 9.53 | 1.04 | 0.81 | 84.2 |

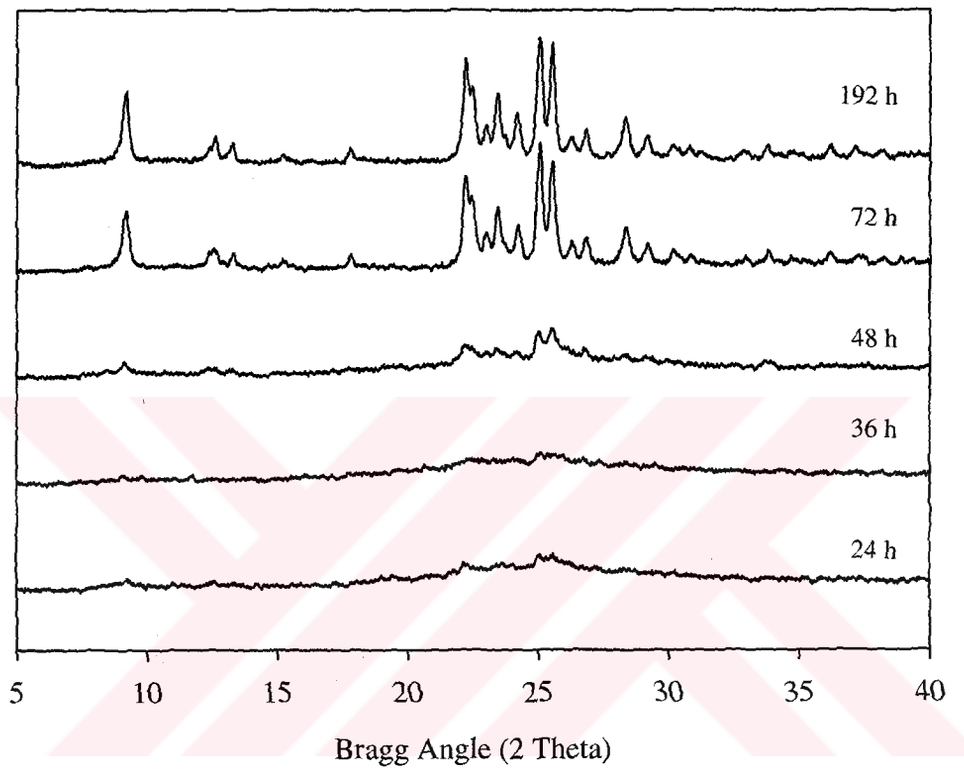


*Figure 4.3 X-Ray Diffraction Patterns of the Samples Synthesized at Different Time Periods from the Batch Composition of 1.85 $Na_2O$. $Al_2O_3$. 20 $SiO_2$. 592 $H_2O$. 19.7 Py at T = 177 °C*

*Table 4.2 Crystallization of ZSM-35 from a Molar Batch Composition of 1.85 $Na_2O$. $Al_2O_3$. 25 $SiO_2$. 592 $H_2O$. 19.7 Py at T = 177 °C*

| Batch Code | Sample Code | Crystallization Time (h) | Crystalline Phases | Weight of Batch (g) | Weight of Product (g) | % Yield | Crystallinity Index | Yield/ Maximum Yield | % Conversion |
|---|---|---|---|---|---|---|---|---|---|
| Z8 | ZC52 | 0 | Amorphous | - | - | - | - | - | - |
| | ZC53 | 36 | ZSM-35 | 26.52 | 2.58 | 9.73 | 1.00 | 0.84 | 84.0 |
| | ZC54 | 48 | ZSM-35 | 31.31 | 2.96 | 9.45 | 1.02 | 0.82 | 83.6 |
| | ZC55 | 168 | ZSM-35 | 27.87 | 2.82 | 10.12 | 1.00 | 0.88 | 88.0 |

*Table 4.3 Crystallization of ZSM-35 from a Molar Batch Composition of 1.85 $Na_2O$. $Al_2O_3$. 15.2 $SiO_2$. 592 $H_2O$. 19.7 Py at T = 177 °C*

| Batch Code | Sample Code | Crystallization Time (h) | Crystalline Phases | Weight of Batch (g) | Weight of Product (g) | % Yield | Crystallinity Index | Yield/ Maximum Yield | % Conversion |
|---|---|---|---|---|---|---|---|---|---|
| Z3 | ZC33 | 0 | Gibbsite Major Amorphous Minor | - | - | - | - | - | - |
| | ZC34 | 15 | Gibbsite Amorphous ZSM-35 Mordenite | 30.94 | 2.33 | 7.53 | 0.50 | 0.94 | 47.0 |
| | ZC35 | 24 | ZSM-35 Major Mordenite Minor | 33.90 | 2.54 | 7.49 | 0.84 | 0.93 | 78.1 |
| | ZC36 | 36 | ZSM-35 Major Mordenite Minor | 35.61 | 2.70 | 7.58 | 0.77 | 0.95 | 73.2 |
| | ZC17 | 48 | ZSM-35 Major Mordenite Minor | 33.96 | 2.61 | 7.69 | 0.92 | 0.96 | 88.3 |
| | ZC18 | 96 | ZSM-35 Major Mordenite Minor | 34.97 | 2.43 | 6.95 | 0.92 | 0.87 | 80.0 |
| | ZC19 | 192 | ZSM-35 Major Mordenite Minor | 36.97 | 2.67 | 7.22 | 0.93 | 0.90 | 83.7 |
| | ZC20 | 288 | ZSM-35 Major Mordenite Minor | 35.46 | 2.71 | 7.64 | 0.96 | 0.95 | 91.2 |

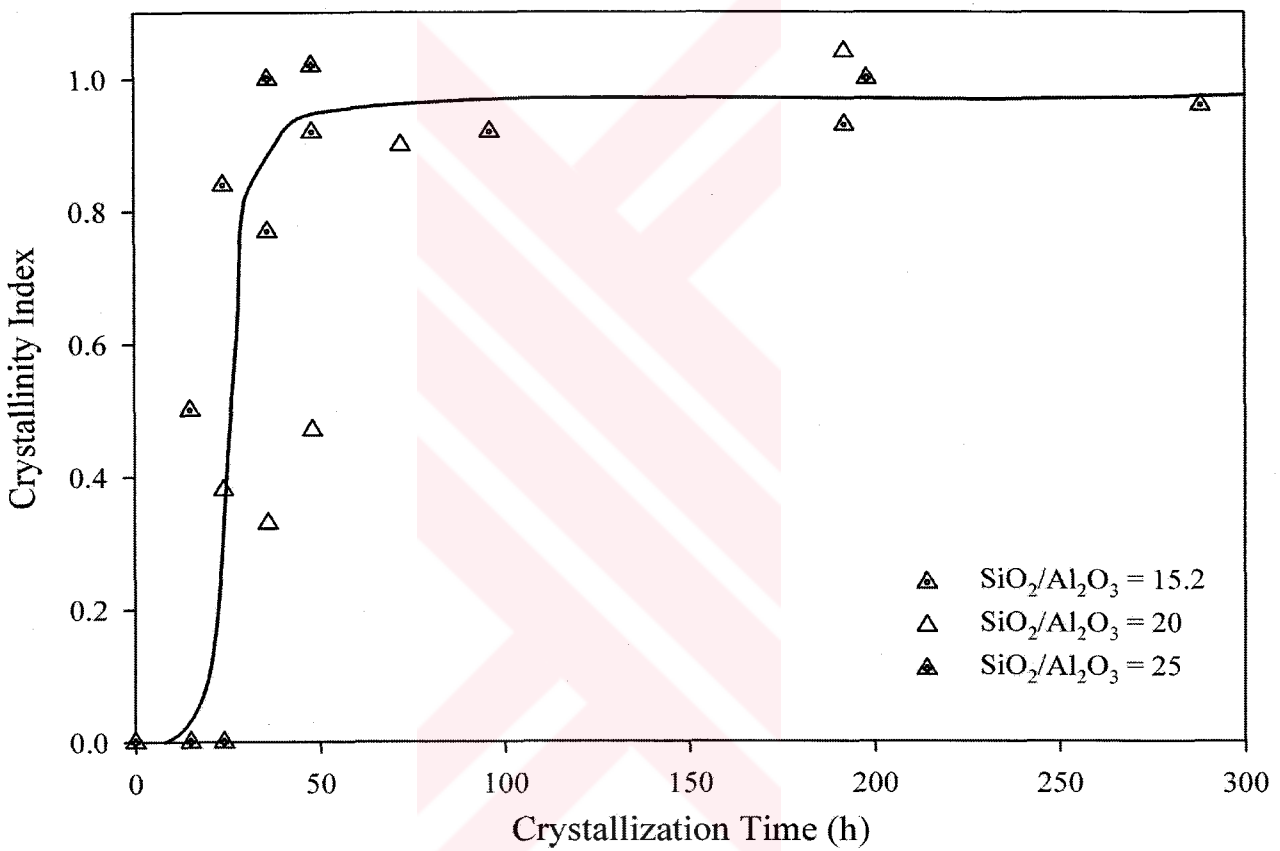


*Figure 4.4 Effect of $SiO_2/Al_2O_3$ Ratio (x) on the Crystallization of ZSM-35 Synthesized at 177 °C from Molar Batch Composition of 1.85 $Na_2O$. $Al_2O_3$. x $SiO_2$. 592 $H_2O$. 19.7 Py*

ZSM-35 synthesis strongly depends on $SiO_2/Al_2O_3$ ratio. Phase purity increases with an increase in this ratio. As it is seen from Table 4.1 and Table 4.2, the experiments performed at $SiO_2/Al_2O_3$ ratio of 20 and 25 at 177 °C and with the template pyrrolidine, single phase ZSM-35 synthesis was achieved. In the experiments performed at lower ratios where $SiO_2/Al_2O_3$ ratio $\leq$ 15.2, mordenite was observed to appear as the impurity phase along with ZSM-35.

$SiO_2/Al_2O_3$ ratio of the batch composition does not have a significant effect on crystallization rate.

### 4.2.2 Crystallization Results of the Experiments Performed at Different Temperatures with Templates Pyrrolidine or Ethylenediamine

The limits of crystallization with respect to temperature were investigated in a range from 150 to 225 °C. The $SiO_2/Al_2O_3$ ratio of the batch composition in these experiments was selected as 20 such that ZSM-35 can be crystallized as a single phase.

The results of the experiments that were performed at 150 °C with the templates pyrrolidine or ethylenediamine are tabulated in Table 4.4 and Table 4.5. The results belonging to the remaining sets are given in Appendix A5. Figure 4.5 shows the effect of template type on the crystallization rate for the samples synthesized at 177 °C and 200 °C. Figure 4.6 shows the effect of temperature on the crystallization rate of the samples synthesized in the presence of ethylenediamine. The effect of temperature on the crystallization rate in the case of pyrrolidine is given in Figure A1. The last figure in this section, Figure 4.7,

gives two sample XRD patterns of ZSM-35 synthesized at 225 °C with two templates.

Both pyrrolidine and ethylenediamine seemed to be effective structure directing agents in ZSM-35 synthesis.

In the experiments performed at temperatures 150, 177 and 200 °C with templates pyrrolidine or ethylenediamine, ZSM-35 was synthesized as a single phase product. At 150 °C synthesis for pyrrolidine and ethylenediamine cases, crystallinity Index, yield and percent conversion data were found to be similar to each other. (Table 4.4, Table 4.5).

In the products of synthesized with pyrrolidine at 177 °C, the crystallization rate was higher than the ones synthesized with ethylenediamine under the same conditions. However, at 200 °C synthesis, the crystallization rate of the products synthesized with ethylenediamine was observed to be higher than the ones synthesized with pyrrolidine (Figure 4.5).

It is observed from Figure 4.6 that an increase in temperature causes a decrease in nucleation period of synthesis and an increase in crystallization rate.

~~At 225 °C, in the~~ experiment performed with pyrrolidine, mordenite was observed as a minor phase along with major phase ZSM-35. But, in the case of template ethylenediamine, ZSM-35 synthesis was achieved without the presence of impurity phases (Figure 4.7) and also in shorter crystallization periods (Table A7, Table A8).

*Table 4.4 Crystallization of ZSM-35 from a Molar Batch Composition of 1.85 $Na_2O$. $Al_2O_3$. 20 $SiO_2$. 592 $H_2O$. 19.7 Py at T = 150 °C*

| Batch Code | Sample Code | Crystallization Time (h) | Crystalline Phases | Weight of Batch (g) | Weight of Product (g) | % Yield | Crystallinity Index | Yield/ Maximum Yield | % Conversion |
|---|---|---|---|---|---|---|---|---|---|
| Z13 | ZC73 | 0 | Amorphous | - | - | - | - | - | - |
| | ZC74 | 24 | Amorphous | - | - | - | - | - | - |
| | ZC75 | 72 | ZSM-35 Amorphous | 29.25 | 1.85 | 6.32 | 0.50 | 0.54 | 27.0 |
| | ZC76 | 108 | ZSM-35 | 27.75 | 2.05 | 7.34 | 0.60 | 0.62 | 37.2 |
| | ZC77 | 192 | ZSM-35 | 31.57 | 2.16 | 6.84 | 0.78 | 0.58 | 45.2 |
| | ZC78 | 240 | ZSM-35 | 31.54 | 2.56 | 8.12 | 0.89 | 0.69 | 61.4 |

*Table 4.5 Crystallization of ZSM-35 from a Molar Batch Composition of 1.85 $Na_2O$. $Al_2O_3$. 20 $SiO_2$. 592 $H_2O$. 19.7 ED at T = 150 °C*

| Batch Code | Sample Code | Crystallization Time | Crystalline Phases | Weight of Batch (g) | Weight of Product (g) | % Yield | Crystallinity Index | Yield/ Maximum Yield | % Conversion |
|---|---|---|---|---|---|---|---|---|---|
| Z17 | ZC106 | 0 | Amorphous | - | - | - | - | - | - |
| | ZC107 | 24 | Amorphous | - | - | - | - | - | - |
| | ZC108 | 36 | Amorphous | - | - | - | - | - | - |
| | ZC109 | 48 | Amorphous Major ZSM-35 Minor | 23.52 | 2.15 | 9.14 | 0.30 | 0.76 | 22.8 |
| | ZC110 | 96 | ZSM-35 Major Amorphous Minor | 24.25 | 1.65 | 6.80 | 0.53 | 0.57 | 30.7 |
| | ZC111 | 144 | ZSM-35 | 24.44 | 1.82 | 7.45 | 0.56 | 0.62 | 34.7 |
| | ZC112 | 240 | ZSM-35 | 25.29 | 2.15 | 8.50 | 0.90 | 0.71 | 63.9 |
| | ZC113 | 480 | ZSM-35 | 30.06 | 2.84 | 9.45 | 0.98 | 0.79 | 77.4 |

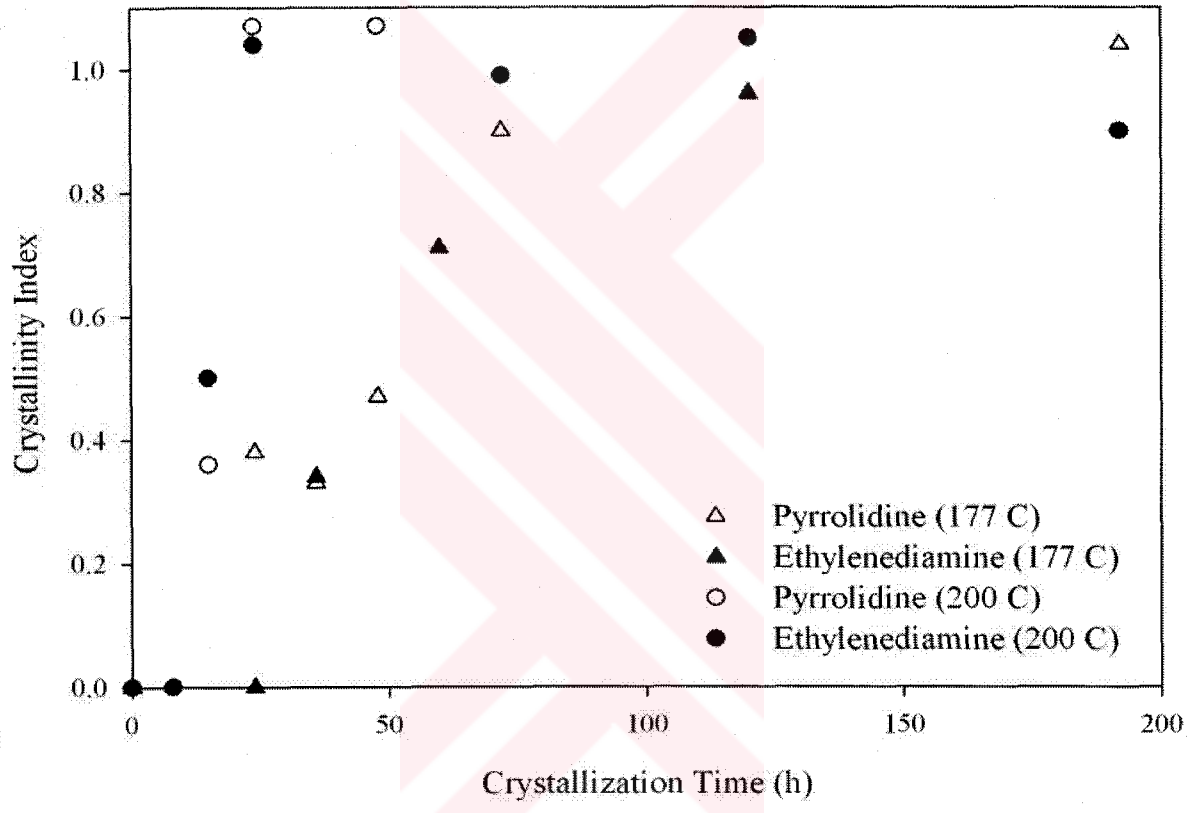


*Figure 4. 5 Effect of Template Type and Temperature on Crystallization of ZSM-35 at 177 and 200 °C from a Molar Batch Composition of 1.85 $Na_2O$. $Al_2O_3$. 20 $SiO_2$. 592 $H_2O$. 19.7 (Py or ED)*

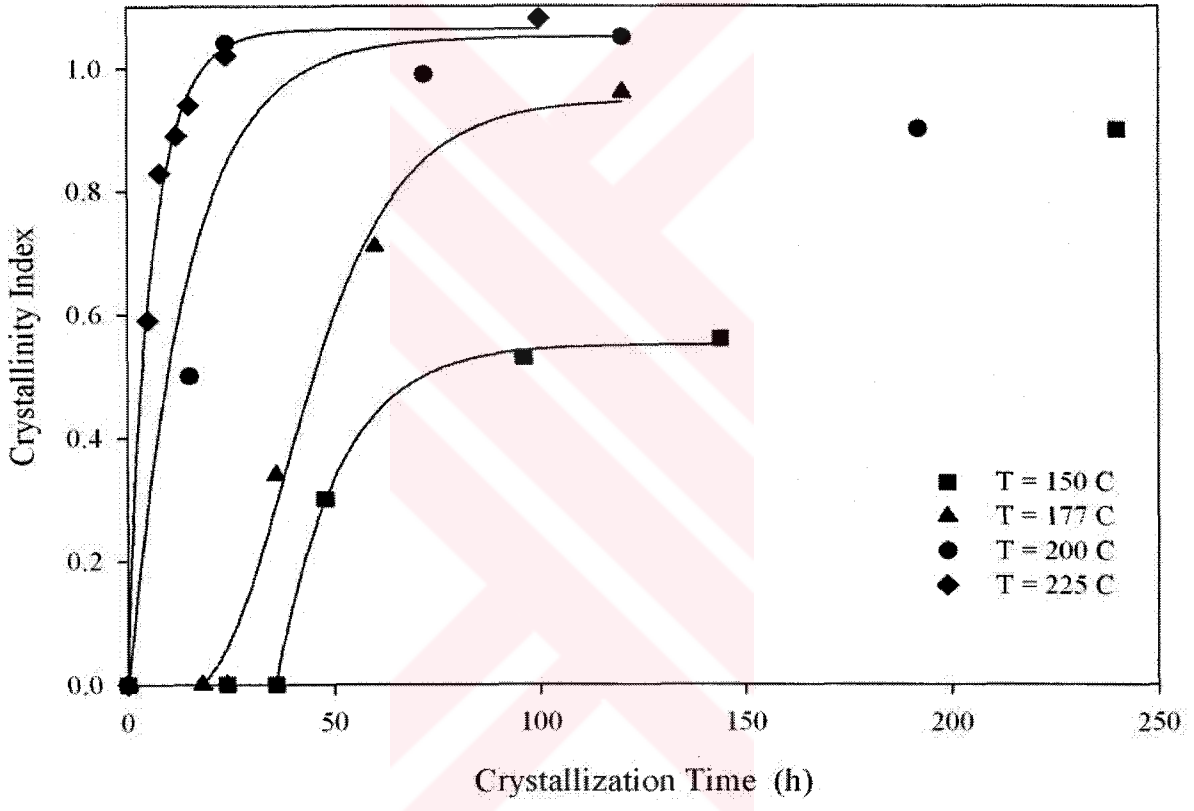


*Figure 4.6 Effect of Temperature on Crystallization of ZSM-35 from a Molar Batch Composition of 1.85 $Na_2O$. $Al_2O_3$. 20 $SiO_2$. 592 $H_2O$. 19.7 ED*

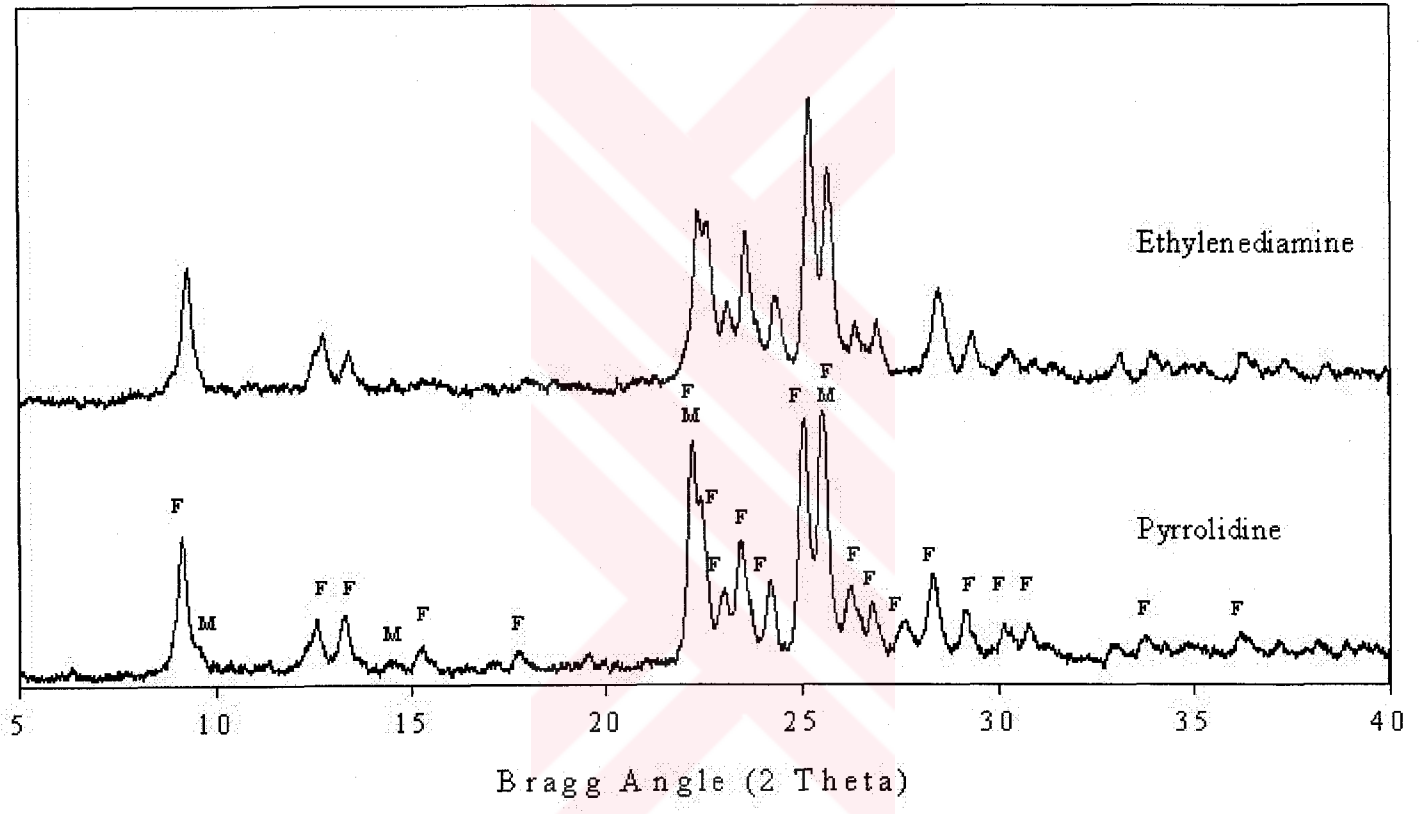


*Figure 4.7 Comparison of the ZSM-35 Samples Synthesized from Molar Batch Composition of 1.85 $Na_2O$. $Al_2O_3$. 20 $SiO_2$. 592 $H_2O$. 19.7 Py or ED (F Denotes ZSM-35, M Denotes Mordenite Phase)*

XRD patterns of the samples synthesized with pyrrolidine and ethylenediamine do not show major differences between the relative peak intensities but, at 150 and 200 °C (Figure B1 and Figure B3), the peaks at 2 theta angle of 22.2 and 22.5 differed in such a way that in XRD pattern of the sample synthesized with pyrrolidine two peaks were observed to overlap. In the other pattern they were seen as two splitted peaks. Such difference was also detected in ZSM-35 patterns given by Robson (1998) and Szostak (1992) that the peaks were seen in separated form whereas in patterns given by Kanno *et al.* (1994) and Borade and Clerafield (1994) these two peaks were overlapped and shown as one broad peak.

One of the autoclaves used for synthesis with ethylenediamine (Batch Code Z17) was left in the oven for 20 days to investigate the stability of crystal phase. The XRD data indicated that ZSM-35 phase is stable under the existing hydrothermal conditions for at least 20 days.

## 4.3 Characterization by SEM

The morphology and the size of the synthesized ZSM-35 crystals were observed by scanning electron microscope. The sample micrographs were shown in the following figures (Figure 4.8- 4.10).

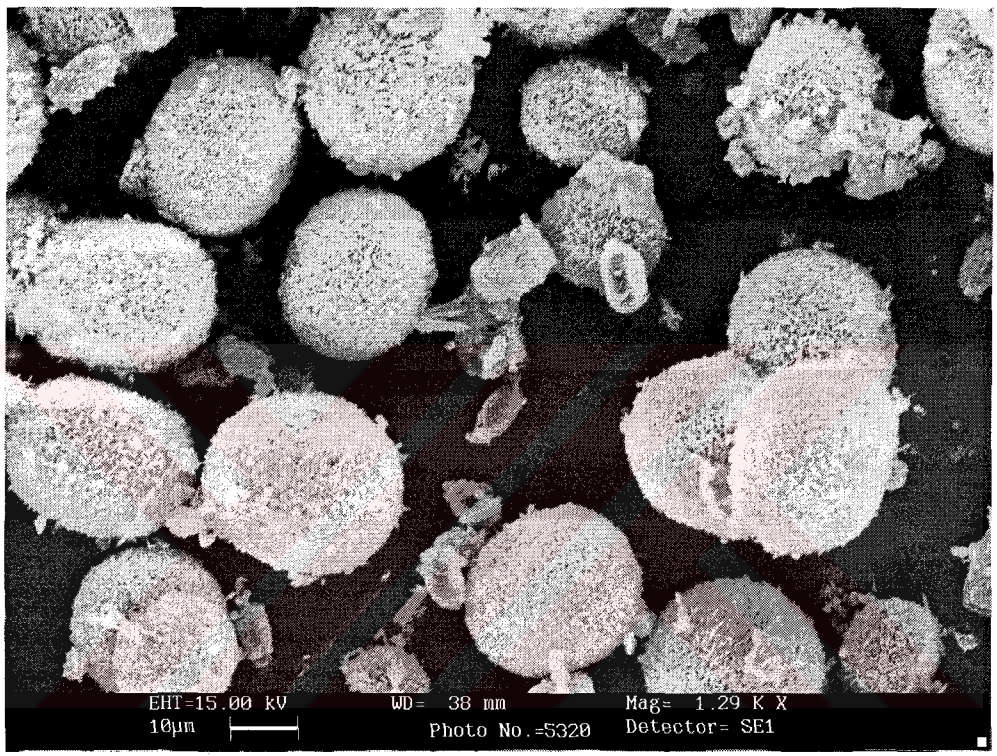


*Figure 4.8 SEM Micrograph of Sample ZC78 (Batch Code Z13, Part 2) Synthesized at 150 °C for 10 Days with Template Pyrrolidine.*

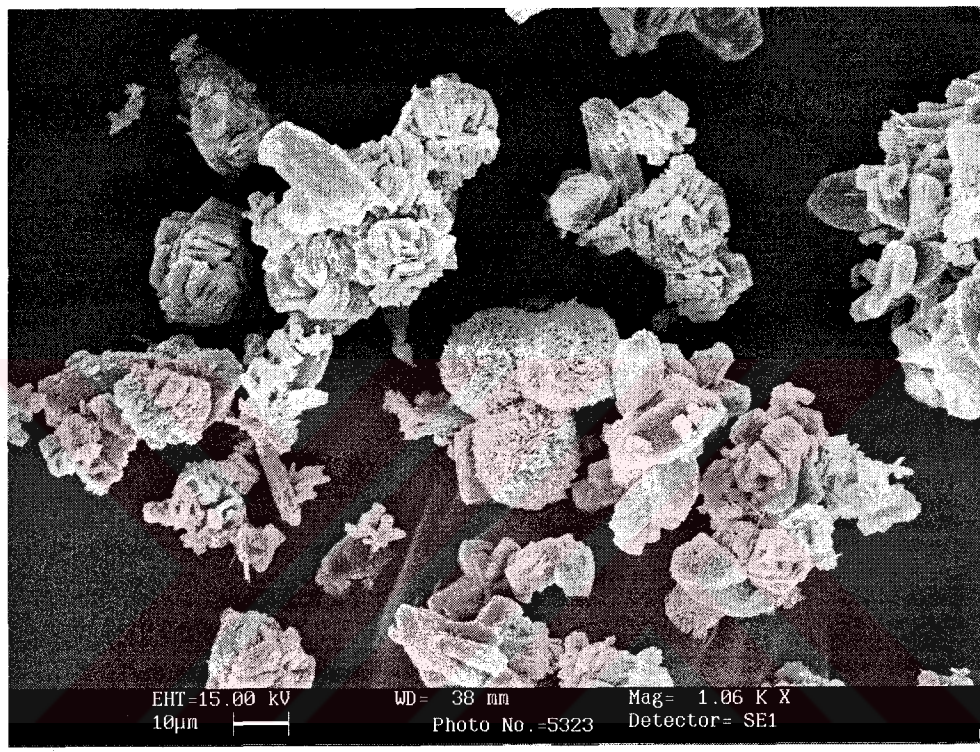


*Figure 4.9 SEM Micrograph of Sample ZC68 (Batch Coded Z11, Part 2) Synthesized at 225 °C for 1 Day with Template Pyrrolidine.*

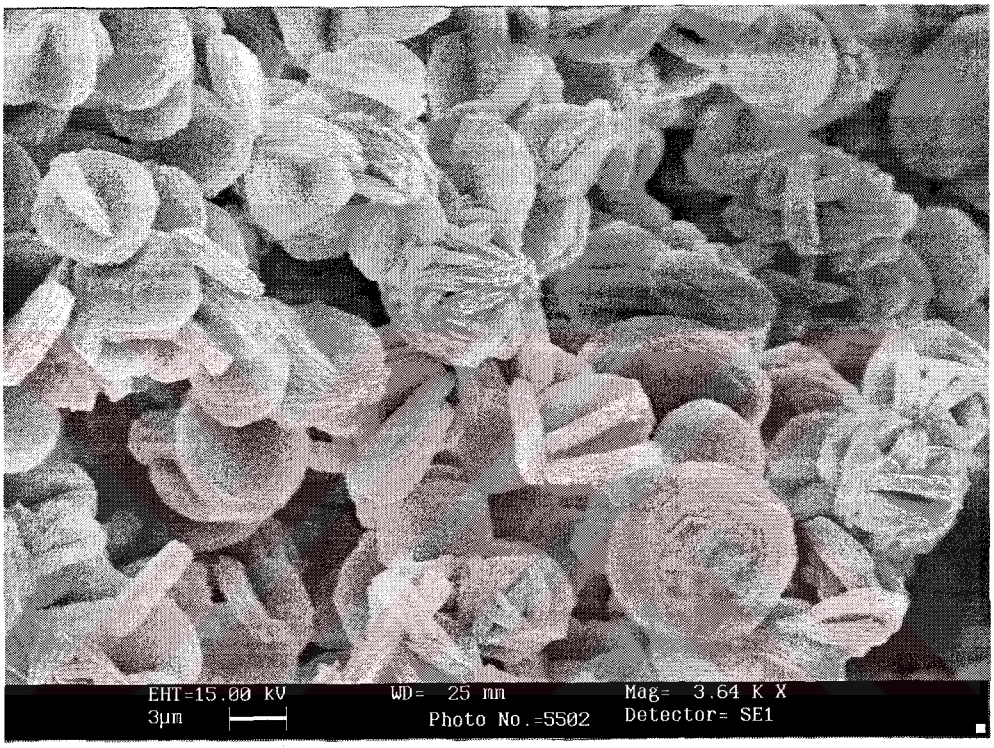


*Figure 4.10 SEM Micrograph of Sample ZC83 (Batch Coded Z14, Part 3) Synthesized at 200 °C for 5 Days with Template Ethylenediamine.*

From Figure 4.8, it is seen that ZSM-35 crystals was formed as spherical crystal agglomerates of 15-20 μm size with individual crystallites smaller than 1 μm. The similar morphology with larger crystal size about 30-40 μm was observed in ZSM-35 sample used in the study of Tütüncü (2003) where the half amount of pyrrolidine used in our study was applied in batch composition.

At 225 °C synthesis, the crystal size was decreased to 5-10 μm. This sample contained minor phase mordenite. Existence of mordenite is not clearly detectable from the micrograph. This sample was also observed to have two different morphologies of ZSM-35. The spherical agglomerates of 5-10 μm in size were dispersed among the platelet shaped crystallites of 5-10 μm in size (Figure 4.9). The platelet shaped crystallites were known for natural ferrierite morphology which was reported to exhibit needle as well as platelet shape crystallites.

Figure 4.10 belongs to ZSM-35 sample synthesized in Part 3 where the syntheses were carried out in the presence of ethylenediamine. The morphology in this case exhibits spherical agglomerates having 5-15 μm size, composed of platelet crystallites. This is a probable morphology as ferrierites are known to have layered structure. It also resembles to the observation reported by Kibby *et al.* (1974) where the crystals of ferrierite was seen to be octagonal platelets stacked like a deck of cards. The similar morphology was reported in the study of Shashikala *et al.* (1991) and Kanno *et al.* (1994) that ferrierite crystallites were in the form of platelets 1-15 μm in size.

The size of the crystallite agglomerates synthesized in the presence of pyrrolidine were observed to decrease with an increase in crystallization

temperature whereas in the case of ethylenediamine the size of crystallite agglomerates increased with increasing the crystallization temperature.

During SEM analysis, EDAX method was applied to some of the samples to determine the $SiO_2/Al_2O_3$ ratio of the products semi-quantitatively. In the previous studies some other $SiO_2/Al_2O_3$ ratio determining methodologies were given. For instance, Jacobs and Martens (1987) showed a plot of $SiO_2/Al_2O_3$ ratio in the synthesis mixture against the same ratio in ferrierite structure. They claimed that up to $SiO_2/Al_2O_3$ ratio of 35 in batch composition, the same ratio in the structure can be obtained and it was possible to synthesize ferrierites in the $SiO_2/Al_2O_3$ range 15 to 35. Suzuki *et al.* (1986) synthesized ZSM-35 with $SiO_2/Al_2O_3$ ratio 24 from a gel of having this ratio 28. Also in the starting batch composition (Robson, 1998) $SiO_2/Al_2O_3$ ratio was 15.2 in synthesis mixture and 13 in zeolite structure. The $SiO_2/Al_2O_3$ ratios in ZSM-35 structure used during the calculations of the maximum yield and conversion were mentioned previously in Section 3.5. Table 4.6 gives the EDAX analysis results and the used $SiO_2/Al_2O_3$ ratios of some synthesized samples. EDAX analyses (Table 4.6) support the argument that $SiO_2/Al_2O_3$ ratios in gel composition and in the structure of the synthesized products are similar.

*Table 4.6 EDAX Analysis Results of the Samples Coded As ZC55, ZC59, ZC17, ZC83 and ZC86*

| Sample Code | Batch Code | $SiO_2/Al_2O_3$ Molar Ratio in Batch Composition | $SiO_2/Al_2O_3$ Molar Ratio in The Product EDAX Results | $SiO_2/Al_2O_3$ Molar Ratio Used in Maximum Yield and Conversion Calculations |
|---|---|---|---|---|
| ZC55 | Z8 | 25 | 19 | 20 |
| ZC59 | Z9 | 10 | 9 | 10 |
| ZC17 | Z3 | 15.2 | 13 | 13 |
| ZC83 | Z14 | 20 | 20 | 20 |
| ZC86 | Z15 | 20 | 20 | 20 |

## 4.4 Characterization by TGA

TGA was applied to the synthesized samples in order to find the template removal temperature of the synthesized ZSM-35 samples and to observe the water desorption amount and weight change in zeolite due to heating. The experiments were carried out under nitrogen or air flow in the temperature range of 30 to 900 °C, with heating rates of 5 and 10 °C/min.

Figure 4.11 (a) and (b) shows that TGA of sample ZC42 (Batch Coded Z5) synthesized with pyrrolidine under nitrogen and air flow with a heating rate of 10 °C/min. Figure 4.12 shows the TGA of the sample ZC83 (Batch Coded Z14, Part 3) synthesized with ethylenediamine under nitrogen flow with a heating rate of 5 °C/min.

It is seen from Figure 4.11 that between room temperature and 200 °C, a weight loss about 1.6 % occurs due to desorption of water. For the sample synthesized with ethylenediamine the water desorption amount was higher and it was about 3%. This value was reported as 1.8 % in the study of Borade and Claerfield (1994) and as 2 % in the study of Gies and Gunawardane (1987).

The weight loss above 200 °C, which amounts to 10-12 %, can be ascribed to desorption and/or decomposition of pyrrolidine or ethylenediamine species from zeolite pores. Pyrrolidine left the zeolite structure at about 530 °C. This observation is in agreement with ZSM-35 sample used in the study of Tütüncü (2003).

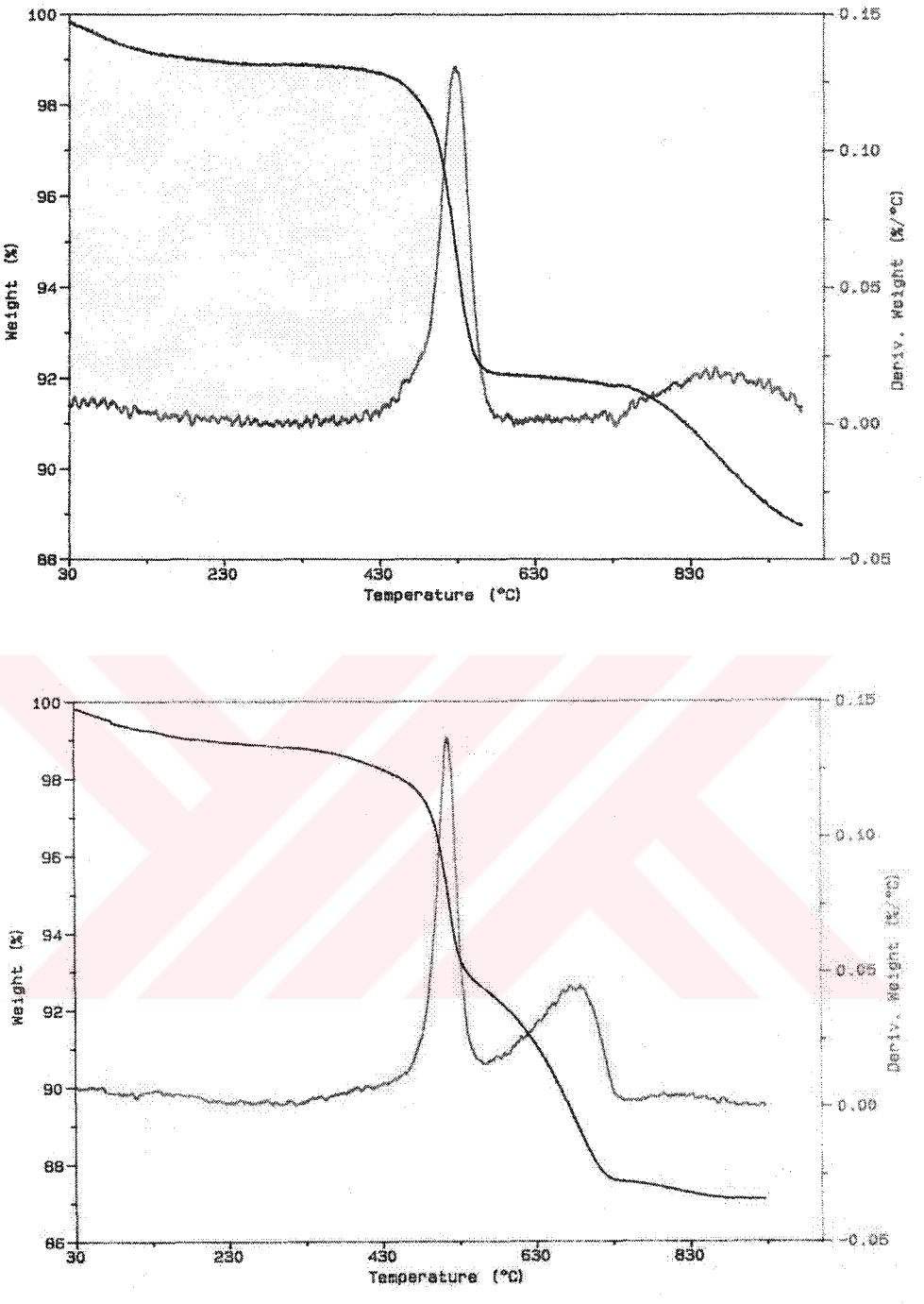


*Figure 4.11 TGA Graphs of the Sample Synthesized with Pyrrolidine (ZC42, Part 1) (a) under Nitrogen Flow (b) under Air Flow*

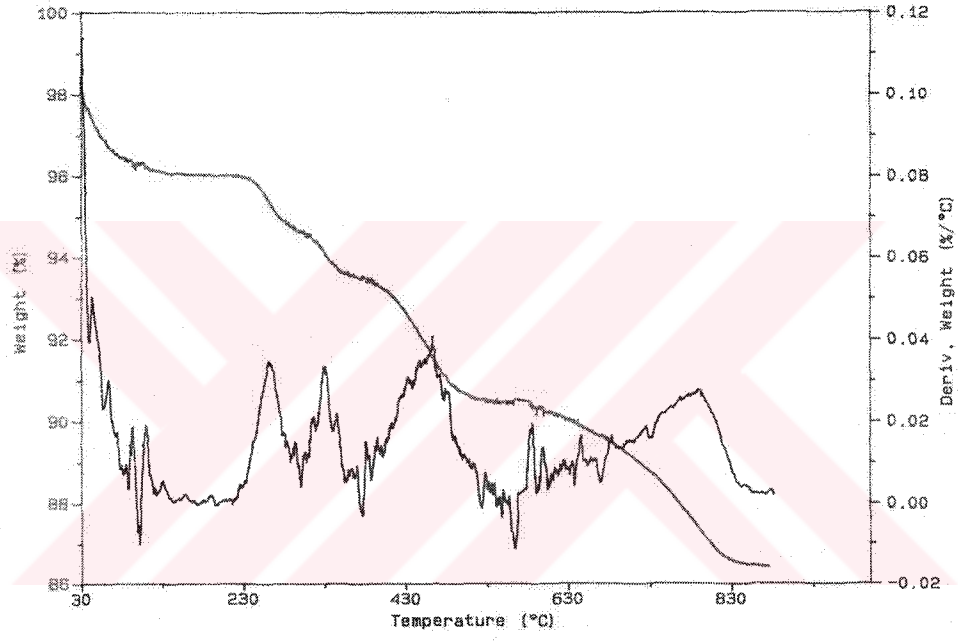


*Figure 4.12 TGA Graph of Sample ZC83 (Part 3) Synthesized with Ethylenediamine under Nitrogen Flow*

Ethylenediamine left the structure in a temperature range from 260 to 800 °C. Similar situation was also implied in the study of Gies and Gunawardane (1987) that the removal of ethylenediamine was given in the temperature range from 350 to 800 °C.

Figure 4.11 (a) and (b) compares the TGA results of the same sample under nitrogen and air flow. In both cases similar results were observed for template removal temperature, water desorption amount and total weight loss. Under nitrogen flow one peak belonging to pyrrolidine removal was observed at about 530 °C. However, under air flow at about 700 °C a second broad peak was observed. This situation probably happened because of volatilization of the coked residuals of pyrrolidine in the structure under air atmosphere.

In Figure 4.11 (a), weight loss was observed to continue at about 900 °C, this situation was clarified in Figure 4.11 (b) that under nitrogen flow as coked organic particles left the structure at higher temperatures than they do under air flow and they imply their existence as weight loss. They would most probably leave the structure above 900 °C in nitrogen flow because in the TGA graph of ZSM-35 sample used in the study of Tütüncü (2003) weight loss increment was seen to be finished at about 950 °C and above this temperature it was stayed at a constant value. In the case of TGA under air flow, after the coked residuals left the structure at about 700 °C, the weight loss was almost stayed constant.

## 4.5 Thermal Stability Test

Thermal stability test was applied in order to obtain the structure breakdown temperature of the synthesized ZSM-35 samples. Samples were treated at

different temperatures in the range of 200 to 1100 °C. The heating rate was 20 °C/min. The changes in the structure of the treated products were observed by XRD analysis and the differences in XRD patterns were investigated.

This test was applied on completely crystallized samples ZC42, ZC71 which were synthesized in the presence of pyrrolidine and ZC81 which was synthesized with ethylenediamine. ZC42 was again scanned by XRD with smear mount before applying heat treatment and its crystallinity index was obtained as 0.95. The crystallinity results of the samples after heat treatments are shown in Table 4.7. The XRD patterns of ZC42 at different treatment temperatures were shown in Figure 4.13.

It was observed from Table 4.7 that the crystallinities of the product were reduced as the treating temperature increased for the samples synthesized with both templates. Also, the intensity of the first peak at 2 theta angle of 9.2 was seemed to be intensified with increasing temperature. The other intensities were observed to decrease relative to each other.

The analyses showed that the structure of the synthesized ZSM-35 samples were stable up even at 1050 °C. At 1100 °C the structure was totally collapsed. This temperature is greater than the ones given in previous studies. For example, the thermal stability of ZSM-35 was reported as 952 °C by Fjellvag *et al.* (1989), as 1000 °C by Gies and Gunawardane (1987), Borade and Clearfield (1994), Kanno *et al.* (1994) and as 1019 °C by Long *et al.* (2000).

*Table 4.7 Thermal Stability Test Crystallinity Results*

| Sample No | Treating Temperature (°C) | Treatment Time (h) | Cyrstallinity Index |
|---|---|---|---|
| ZC42-1 | 200 | 0.5 | 0.88 |
| ZC42-2 | 300 | 0.5 | 0.85 |
| ZC42-3 | 400 | 0.5 | 0.67 |
| ZC42-4 | 500 | 0.5 | 0.71 |
| ZC42-5 | 600 | 0.5 | 0.76 |
| ZC42-6 | 700 | 0.5 | 0.57 |
| ZC42-7 | 800 | 0.5 | 0.81 |
| ZC42-8 | 900 | 0.5 | 0.59 |
| ZC42-9 | 950 | 0.5 | 0.71 |
| ZC42-10 | 950 | 1.0 | 0.69 |
| ZC42-11 | 950 | 2.0 | 0.69 |
| ZC42-12 | 1000 | 0.5 | 0.70 |
| ZC42-13 | 1000 | 1.0 | 0.52 |
| ZC42-14 | 1000 | 2.0 | 0.42 |
| ZC42-15 | 1050 | 0.5 | 0.68 |
| ZC42-16 | 1050 | 1.0 | 0.80 |
| ZC42-17 | 1050 | 2.0 | 0.55 |
| ZC42-18 | 1100 | 2.0 | 0.00 |
| ZC71-1 | 600 | 2.0 | 0.67 |
| ZC71-2 | 900 | 2.0 | 0.65 |
| ZC71-3 | 1050 | 2.0 | 0.51 |
| ZC81-1 | 600 | 2.0 | 0.66 |
| ZC812 | 900 | 2.0 | 0.63 |
| ZC81-3 | 1050 | 2.0 | 0.39 |

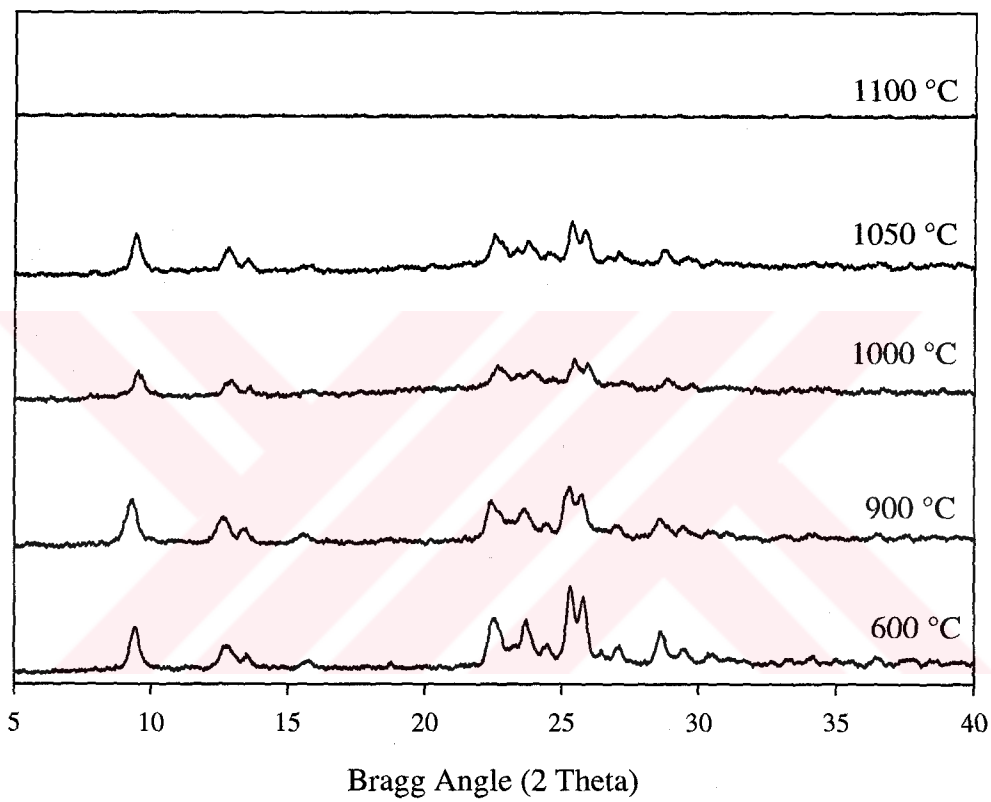


*Figure 4.13 Comparison of XRD Scans of Sample ZC42 Treated at Temperatures 600 (0.5 h), 900 (0.5 h), 1000 (2 h), 1050 (2 h) and 1100 °C (2 h)*

## 4.6 Sorption Capacity Measurements

Total sorption volume of ZSM-35 was reported by Jacobs and Martens (1987) as 0.1561 $cm^3/g$ of which 0.1000 $cm^3/g$ is the pore volume of 10 membered rings. Previous studies (Harrison *et al.* (1987) and Tütüncü (2003)) has shown that that methanol can penetrate both 10 and 8 membered ring channels of ferrierite and limiting methanol sorption capacities can be taken as an indication of purity of the samples. For this purpose, equilibrium sorption capacities of some high crystallinity samples of were measured in a gravimetric sorption apparatus. Measurements were carried out at 0 and 25 °C and at different relative pressures ($P/P_0$) where P is the equilibrium pressure and $P_0$ is the vapor pressure of methanol at 0 °C ( 28.12 mmHg) and 25 °C (109.86 mmHg) (Perry and Green, 1999). Volumetric methanol sorption capacities are calculated from the weight absorbed assuming that methanol exists as a normal liquid at the temperature of adsorption. Liquid densities of methanol at 0 °C and 25 °C are taken as 0.8102 and 0.7893 $g/cm^3$ respectively (Perry and Green, 1999). Table 4.8 gives the data of this study and some previous studies for comparison. It is shown that sorption under comparable conditions, ZSM-35 samples synthesized by templates pyrrolidine and ethylenediamine have high volumetric sorption capacities approaching to the theoretical intracrystalline volume of ZSM-35. The volumetric sorption capacities calculated at 0 °C are higher than those calculated at 25 °C under comparable relative pressures. This is probably due to more favorable packing of methanol molecules in the channels of ZSM-35 at the lower temperature.

*Table 4.8 Comparison of Methanol Sorption Capacities of Synthesized ZSM-35 Samples with Previous Studies*

| Reference | T (°C) | $P/P_0$ | Sorbent | Absorbed Volume of Methanol ($cm^3/g$) | % Filling of Total Pore Volume |
|---|---|---|---|---|---|
| This Study | 25 | 0.5 | Na ZSM-35 (Py) | 0.1380 | 88.4 |
| | 0 | 0.5 | Na ZSM-35 (Py) | 0.1495 | 95.8 |
| | 0 | 0.4 | Na ZSM-35 (ED) | 0.1363 | 87.3 |
| | 0 | 0.8 | Na ZSM-35 (ED) | 0.1518 | 97.2 |
| Harrison *et al.* (1987) | 23 | 0.5 | H Ferrierite | 0.1357 | 86.9 |
| Öztin (1997) | 25 | 0.5 | Na ZSM-35 | 0.1218 | 78 |
| Karslı *et al.* (2003) | 25 | 0.5 | H Ferrierite | 0.1200 | 77 |
| Tütüncü (2003) | 23 | 0.5 | Na ZSM-35 | 0.1150 | 73.7 |
| Long *et al.* (2000) | 25 | 0.6 | Na,K ZSM-35 | 0.0850 | 54.5 |
| Kıvanç *et al.* (1992) | 25 | 0.5 | Na Ferrierite | 0.0792 | 50.7 |

# CHAPTER 5

# CONCLUSIONS

1. From the experiments performed in the presence of template pyyrolidine at $SiO_2/Al_2O_3$ ratio 25 at 177 °C and the experiments performed at $SiO_2/Al_2O_3$ ratio of 20, at temperatures 150, 177 and 200 °C, ZSM-35 was synthesized as a single phase product.

   At 225 °C, mordenite was observed as a minor phase along with major phase ZSM-35.

2. From the experiments performed in the presence of template ethylenediamine at $SiO_2/Al_2O_3$ ratio of 20, at temperatures 150, 177, 200 and 225 °C, pure phase ZSM-35 was synthesized.

3. ZSM-35 crystals synthesized with pyrrolidine were observed to be spherical crystal agglomerates of 15-20 μm size with individual crystallites smaller than 1 μm. The morphology of the products synthesized with ethylenediamine at temperatures exhibits spherical agglomerates composed of platelet crystallites.

4. The thermal stability analyses showed that the structure of the synthesized ZSM-35 samples is stable up even at 1050 °C. At 1100 °C the structure totally collapses.
5. The volumetric sorption capacities for methanol at 0 and 25 °C approached to the theoretical pore volume reported for ZSM-35.

## 5.1 Recommendations

In this study the crystallizatiıon field of ZSM-35 was investigated by changing the synthesis parameters in certain ranges. This investigation can further be extented by enlarging the parameter ranges or by applying different synthesis parameters such as the $H_2O$ amount, the template amount or $Na_2O/Al_2O_3$ ratio to see their effects on the synthesis of ZSM-35.

The methanol sorption capacity of the synthesized samples can be measured at higher temperatures in order to observe the effect of temperature on the sorption capacity. Also, sorption capacity measurements can be performed in hydrogen form ZSM-35 to observe the capacity differences in sodium and hydrogen forms of ZSM-35. The adsorptive properties of ZSM-35 can further be extented by using different sorbates.

# REFERENCES


Araya A., Lowe B. M., 'A Partial Determination of the Stability Fields of Ferrierite and Zeolites ZSM-5, ZSM-48, and NU-10 in the $K_2O$- $Al_2O_3$- $SiO_2$- $NH_2[CH_2]$ $6NH_2$ System', J. Chem. Res. 6, 192-193, 1985.

Barrer R. M., Marshall D., 'Hydrothermal Chemistry of Silicates. Part XIII. Synthetic Barium Aluminosilicates', J., Amer. Mineral. 50, 484, 1965.

Breck D.W., 'Zeolite Molecular Sieves', Wiley, Newyork, 1974.

Borade, R.B., Clearfield, A., 'Synthesis of ZSM-35 Using Trimethylcetyl-ammonium Hydroxide as a Template', Zeolites 14, 458-461, 1994.

Cormier W. E., Sand L. B., 'Synthesis and Metastable Phase-Transformations of Na- Ferrierites, Na,K- Ferrierites and K-Ferrierites', Amer. Mineral. 52, 1259-1266, 1976.

Çulfaz A., Yılmaz K.A., 'Synthesis and Characterization of Ferrierite', Crystal Res. & Technol. 20, 11-19, 1985.

Elvers B., Hawkins S., ed, 'Ullmann's Encylopedia of Industrial Chemistry', Vol. A 28, 475-504, Weinheim, New York, 1996.

Fjellvag H., Lillerud K.P., Norby P., Sorby K. 'Structural Properties on Some Ferrierite-Type Zeolites', Zeolites 9, 1989.

Forbes N.R., Rees L.V., 'The Synthesis of Ferrierite, ZSM-5 and Theta-1 in the Presence of Diethanolamine: Experimental', Zeolites 15, 444-451, 1995.

Gies H., Gunawardene R. P., 'One-Step Synthesis, Properties and Crystal Structure of Aluminum-Free Ferrierite', Zeolites 7, 442-445, 1987.

Harrison I.D., Leach H.F., Whan D.A., 'Comparison of Shape Selective Properties of Ferrierite, ZSM-5 and ZSM-11, Zeolites 7, 21-27, 1987.

Jacobs P.A., Martens J.A., 'High Silica Zeolites of the Ferrierite Family' Stud. Surf. Sci. Catal. 33, 217-232, 1987.

Kanno N., Miyake M., Sato M., 'Synthesis of Ferrierite, ZSM-48 and ZSM-5 in Glycerol Solvent', Zeolites 14, 625-628, 1994.

Karslı H., Çulfaz A., Yücel H., 'Sorption Properties of Synthetic Ferrierite', Chemical Engineering Communications, 190, 643-704, 2003.

Kerr I.S., ' Structure of Ferrierite', Nature 210, London, 294, 1967.

Kibby C. L. , Perrotta A. J., Massoth F. E., 'Composition and Catalytic Properties of Synthetic Ferrierite', J. Catal. 35, 256-272, 1974.

Kıvanç, A.N., 'Adsorption Properties of Synthetic and Natural Ferrierite', M.Sc. Thesis, METU, Ankara, 1992.

Long Y., Ma M., Sun Y., Jiang H., 'Synthesis, Ion-exchange, Structural Characterization and Adsorption of K,Na-FER Type Zeolite', Journal of Inclusion Phenomena and Macrocyclic Chemistry 37, 103-120, 2000.

Morimoto N., Takatsu K., Sugimoto M., US Patent 4,578,259, 1986.

Öztin A., 'Sorption Properties of a High Silica Zeolite ZSM-35', M.Sc. Thesis, METU, Ankara, 1997.

Perry R.H., Green D.W., ed., 'Perry's Chemical Engineering Handbook', 7th Ed., 2-41, 2-70, 2-111, McGraw-Hill, New York, 1999.

Plank C.J., Rosinski E.J., Rubin M.K., US Pat. 4,016,245, assigned to Mobil Oil Corp., 1977.

Robson H., ' How to Read a Patent', Microporous Materials 22, 551-666, 1998.

Seddon D., Whittam T.V.E., Patent B-55, 529, 1985.

Shashikala J.R., Satyanarayana C.V.V., Chakrabarty D.K., 'Shape Selective Catalysis by ZSM-35 Zeolites, Disproportion of Ethylbenzene and Isomerization of m-Xylene', Appl. Catal 69, 177-186, 1991.

Suzuki K., Kiyozumi Y., Shin S., Fjuisawa K., Watanabe H., Saita K., Noguchi K., 'Zeolite Synthesis in the System Pyrrolidine-$Na_2O$-$Al_2O_3$-$SiO_2$-$H_2O$', Zeolites 6, 290-298, 1986.

Szostak R., 'Handbook of Molecular Sieves', Van Nostrand Reinhold, New York, 1992.

Tütüncü G., 'Sorption Properties of High Silica Zeolites', M.Sc. Thesis, METU, Ankara, 2003.

Valyocsic E.W., Rollmann L.D., ' Diamines as Template in Zeolite Crystallization', Zeolites 5, 123-125, 1985.

Vaughan P.A., 'The Crystal Structure of the Zeolite Ferrierite', Acta Crystallogr. 21, 983, 1966.

Wenyang X., Jianquan L.,Wenyuan L., Huiming Z., Bingchang L., 'Nonaqueous Synthesis of ZSM-35 and ZSM-5', Zeolites 9 , 468-473, 1989.

Whittam T.V.E., Patent A-103, 981, 1984.

# APPENDIX A

# SYNTHESIS CALCULATIONS

## A.1 Crystallinity Index Calculation

Crystallinity index of the samples were calculated from the following equation,

$$\text{Crystallinity Index} = \frac{\sum_{n=1}^{20} I_{n,s}}{\sum_{n=1}^{20} I_{n,0}}$$

$I_{n,s}$ represents the peak intensity data of the synthesized sample and $I_{n,0}$ represents the peak intensity data of the reference sample. In order to form a reference sample, 20 major peaks were selected from the XRD patterns of highly crystalline, pure ZSM-35 samples. The intensity data of these 20 peaks were summed up for all the samples. These summations were then averaged for determining the intensity summation data of 20 peaks of the reference sample. The crystallinity index calculation method applied on the 9 selected samples is shown in Table A1.

*Table A.1 Intensity Data and Crystallinity Index Calculation of the Most Crystalline ZSM-35 Samples*

| Peak No | Bragg Angle | Intensity (I) | | | | | | | | | | |
|---|---|---|---|---|---|---|---|---|---|---|---|---|
| | | ZC41 | ZC54 | ZC65 | ZC68 | ZC71 | ZC83 | ZC86 | ZC92 | ZC105 | AVG | RI |
| 1 | 9.28 | 800 | 1180 | 850 | 1000 | 1040 | 1100 | 950 | 1000 | 1000 | 991±110 | 53 |
| 2 | 12.52 | 350 | 400 | 350 | 370 | 450 | 450 | 470 | 450 | 450 | 416±45 | 22 |
| 3 | 13.39 | 250 | 300 | 350 | 400 | 350 | 320 | 350 | 250 | 300 | 319±47 | 17 |
| 4 | 15.38 | 100 | 200 | 200 | 200 | 200 | 170 | 120 | 150 | 120 | 162±39 | 9 |
| 5 | 17.92 | 200 | 200 | 200 | 200 | 240 | 170 | 120 | 150 | 100 | 176±42 | 9 |
| 6 | 22.34 | 1350 | 1450 | 1420 | 1550 | 1560 | 1250 | 1250 | 1100 | 1250 | 1353±146 | 72 |
| 7 | 22.62 | 1200 | 1250 | 1070 | 1150 | 1260 | 1250 | 1170 | 1100 | 1100 | 1172±68 | 62 |
| 8 | 23.10 | 500 | 550 | 520 | 500 | 600 | 600 | 550 | 500 | 580 | 544±39 | 29 |
| 9 | 23.60 | 900 | 1000 | 950 | 850 | 1020 | 1250 | 1100 | 1000 | 1050 | 1013±110 | 54 |
| 10 | 24.32 | 500 | 650 | 580 | 550 | 590 | 650 | 620 | 550 | 630 | 591±48 | 31 |
| 11 | 25.23 | 1850 | 1900 | 1690 | 1750 | 1900 | 2050 | 2060 | 1950 | 1750 | 1878±124 | 100 |
| 12 | 25.67 | 1520 | 1650 | 1800 | 1800 | 1750 | 1700 | 1550 | 1550 | 1670 | 1666±101 | 89 |
| 13 | 26.29 | 270 | 400 | 400 | 500 | 360 | 350 | 450 | 350 | 350 | 381±63 | 20 |
| 14 | 26.94 | 400 | 450 | 430 | 400 | 470 | 390 | 450 | 350 | 350 | 410±41 | 22 |
| 15 | 28.52 | 500 | 600 | 600 | 600 | 650 | 650 | 700 | 650 | 700 | 628±58 | 33 |
| 16 | 29.38 | 300 | 320 | 310 | 350 | 400 | 400 | 370 | 350 | 450 | 361±46 | 19 |
| 17 | 30.26 | 150 | 250 | 230 | 350 | 220 | 200 | 230 | 250 | 200 | 231±51 | 12 |
| 18 | 30.65 | 100 | 150 | 230 | 250 | 220 | 170 | 170 | 200 | 200 | 188±43 | 10 |
| 19 | 33.98 | 150 | 150 | 150 | 150 | 220 | 200 | 200 | 200 | 220 | 182±30 | 10 |
| 20 | 36.33 | 120 | 100 | 150 | 150 | 220 | 200 | 200 | 200 | 220 | 173±42 | 9 |
| $\sum_{n=1}^{20} I_{n,s}$ | | 11510 | 13150 | 12480 | 13070 | 13720 | 13520 | 13080 | 12300 | 12690 | 12836±637 | - |
| Crystallinity Index $CI = \frac{\sum_{n=1}^{20} I_{n,s}}{\sum_{n=1}^{20} I_{n,0}}$ | | 0.90 | 1.03 | 0.97 | 1.02 | 1.07 | 1.05 | 1.02 | 0.96 | 0.99 | 1.00±0.05 | - |

For determining crystallinity indices of the samples having competing phase mordenite in their structure, a similar method was applied on 5 peaks which are not overlapping or existing very near to the mordenite peaks in XRD pattern. The intensity summation of both samples were calculated for only the 5 selected peaks. The crystallinity index of the pure sample was calculated by dividing the intensity summation of 20 peaks to the same value of the reference sample as described in Table A1. The crystallinity index of the two phase samples were calculated by dividing the intensity summation of 5 peaks to the intensity summation of 5 peaks of the pure phase sample (ZC92). Here, pure phase sample was used as a new reference having crystallinity index of 0.96. Sample calculation for this case is shown in Table A2.

*Table A.2 Intensity Data and Crystallinity Index Calculation of ZSM-35 Samples Having Competing Phase Mordenite*

| **Peak No** | **Bragg Angle** | **Intensity** | |
|---|---|---|---|
| | | ZC59 | ZC92 |
| 2 | 12.52 | 230 | 450 |
| 3 | 13.39 | 100 | 250 |
| 5 | 17.92 | 100 | 150 |
| 10 | 24.20 | 450 | 550 |
| 14 | 26.94 | 150 | 350 |
| $\sum_{n=1}^{5} I_{n,s}$ | | 1030 | 1750 |
| Crystallinity Index | | $\frac{1030}{1750} \times 0.96 = 0.57$ | 0.96 |

## A.2 Yield Calculation

In the sample calculations of % yield, maximum yield and % conversion, pure phase ZSM-35 sample ZC92 (Batch Code Z16) was used. It was synthesized at the $SiO_2/Al_2O_3$ ratio of 20, at 177 °C for 120 h.

Weight of Batch = 34.35 g

Weight of product = 2.52 g

$$\% \text{ Yield} = \frac{\text{Weight of Product (g)}}{\text{Weight of Batch (g)}} \times 100$$

$$\% \text{ Yield} = \frac{2.52 \text{ g}}{34.35 \text{ g}} \times 100 = 7.33 \%$$

## A.3 Maximum Yield Calculation

Sample batch composition for ZSM-35 synthesis:

1.85 $Na_2O$. $Al_2O_3$. 20 $SiO_2$. 592 $H_2O$. 19.7 ED

In maximun yield calculations all the reactants were assumed to stay in solid phase product during removal from the autoclaves.

Molecular Weights of Components (g/gmole):

**$Na_2O$** 61.99

**$Al_2O_3$** 101.96

**$SiO_2$** 60.09

**$H_2O$** 18.01

**ED** (Ethylenediamine) 59.8

Weight of Batch :

$$61.99 \times 1.85 + 101.96 + 60.09 \times 20 + 18.01 \times 592 + 59.8 \times 19.7 = 13258.4 \text{ g}$$

Formula ZSM-35 (EDAX) :

$$Na_2O.\ Al_2O_3.\ 20\ SiO_2$$

Formula Weight of ZSM-35 (Water and Template Free):

$$61.99 + 101.96 + 60.09 \times 20 = 1365.75 \text{ g}$$

The amount of water and template in zeolite structure were determined from TGA results as 14 %.

Formula Weight of ZSM-35 = 1365.75/ 0.86 = 1588.08 g

Maximum yield per 100 g Batch:

$$\text{Maximum Yield} = 100 \text{ g Batch} \times \frac{1 \text{ mole Batch}}{13258.4 \text{ g}} \times \frac{1 \text{ mole } Al_2\ O_3}{1 \text{ mole Batch}} \times \frac{1 \text{ mole ZSM-35}}{1 \text{ mole } Al_2\ O_3} \times \frac{1588.08 \text{ g}}{1 \text{ mole ZSM-35}}$$

$$= 11.98$$

## A.4 Conversion Calculation

In this sample, ZC92, $Al_2O_3$ or $SiO_2$ can be defined as the limiting reactant since both of them have the same molar amount in batch composition and in the structure of the product

$$\% \text{ Conversion} = \frac{\text{Yield}}{\text{Maximum Yield}} \times \text{Crystallinity Index}$$

$$\% \text{ Conversion} = \frac{7.33}{11.98} \times 0.96 \times 100 = 58.7\ \%$$

# A.5 Crystallinity Results

*Table A.3 Crystallization of ZSM-35 from a Molar Batch Composition of 1.85 $Na_2O$. $Al_2O_3$. 10 $SiO_2$. 592 $H_2O$. 19.7 Py at T = 177 °C*

| Batch Code | Sample Code | Crystallization Time (h) | Crystalline Phases | Weight of Batch (g) | Weight of Product (g) | % Yield | Crystallinity Index | Yield/ Maximum Yield | % Conversion |
|---|---|---|---|---|---|---|---|---|---|
| Z9 | ZC56 | 0 | Amorphous | - | - | - | - | - | - |
| | ZC57 | 36 | Amorphous Major ZSM-35 Minor | 28.35 | 1.39 | 4.90 | 0.36 | 0.71 | 25.6 |
| | ZC58 | 48 | ZSM-35 Mordenite | 30.60 | 1.58 | 5.16 | 0.57 | 0.75 | 42.8 |
| | ZC59 | 168 | ZSM-35 Mordenite | 30.25 | 1.68 | 5.55 | 0.57 | 0.80 | 45.6 |

*Table A.4 Crystallization of ZSM-35 from a Molar Batch Composition of 1.85 $Na_2O$. $Al_2O_3$. 20 $SiO_2$. 592 $H_2O$. 19.7 ED at T = 177 °C*

| Batch Code | Sample Code | Crystallization Time (h) | Crystalline Phases | Weight of Batch (g) | Weight of Product (g) | % Yield | Crystallinity Index | Yield/ Maximum Yield | % Conversion |
|---|---|---|---|---|---|---|---|---|---|
| Z16 | ZC87 | 0 | Amorphous | - | - | - | - | - | - |
| | ZC88 | 18 | Amorphous ZSM-35 | - | - | - | - | - | - |
| | ZC89 | 24 | Amorphous ZSM-35 | - | - | - | - | - | - |
| | ZC90 | 36 | Amorphous ZSM-35 | 30.17 | 2.88 | 9.38 | 0.34 | 0.78 | 26.5 |
| | ZC91 | 60 | ZSM-35 | 30.00 | 2.56 | 8.53 | 0.71 | 0.71 | 50.4 |
| | ZC92 | 120 | ZSM-35 | 34.35 | 2.52 | 7.33 | 0.96 | 0.61 | 58.7 |

*Table A.5 Crystallization of ZSM-35 from a Molar Batch Composition of 1.85 $Na_2O$. $Al_2O_3$. 20 $SiO_2$. 592 $H_2O$. 19.7 Py at T = 200 °C*

| Batch Code | Sample Code | Crystallization Time (h) | Crystalline Phases | Weight of Batch (g) | Weight of Product (g) | % Yield | Crystallinity Index | Yield/ Maximum Yield | % Conversion |
|---|---|---|---|---|---|---|---|---|---|
| Z12 | ZC69 | 8 | Amorphous | - | - | - | - | - | - |
| | ZC70 | 15 | Amorphous ZSM-35 | 26.78 | 2.45 | 9.12 | 0.36 | 0.77 | 27.7 |
| | ZC71 | 24 | ZSM-35 | 27.52 | 2.27 | 8.25 | 1.07 | 0.70 | 74.9 |
| | ZC72 | 48 | ZSM-35 | 27.61 | 2.49 | 9.02 | 1.07 | 0.77 | 82.3 |

*Table A.6 Crystallization of ZSM-35 from a Molar Batch Composition of 1.85 $Na_2O$. $Al_2O_3$. 20 $SiO_2$. 592 $H_2O$. 19.7 ED at T = 200 °C*

| Batch Code | Sample Code | Crystallization Time (h) | Crystalline Phases | Weight of Batch (g) | Weight of Product (g) | % Yield | Crystallinity Index | Yield/ Maximum Yield | % Conversion |
|---|---|---|---|---|---|---|---|---|---|
| Z14 | ZC79 | 0 | Amorphous | - | - | - | - | - | - |
| | ZC80 | 15 | Amorphous ZSM-35 | 30.42 | 2.63 | 8.65 | 0.50 | 0.72 | 36 |
| | ZC81 | 24 | ZSM-35 | 29.04 | 2.46 | 8.47 | 1.04 | 0.71 | 73.8 |
| | ZC82 | 72 | ZSM-35 | 29.00 | 2.48 | 8.55 | 0.99 | 0.71 | 70.3 |
| | ZC83 | 120 | ZSM-35 | 32.48 | 2.74 | 8.44 | 1.05 | 0.71 | 74.5 |
| | ZC84 | 192 | ZSM-35 | 29.24 | 1.89 | 6.46 | 0.90 | 0.54 | 48.6 |

*Table A.7 Crystallization of ZSM-35 from a Molar Batch Composition of 1.85 $Na_2O$. $Al_2O_3$. 20 $SiO_2$. 592 $H_2O$. 19.7 Py at T = 225 °C*

| Batch Code | Sample Code | Crystallization Time (h) | Crystalline Phases | Weight of Batch (g) | Weight of Product (g) | % Yield | Crystallinity Index | Yield/ Maximum Yield | % Conversion |
|---|---|---|---|---|---|---|---|---|---|
| Z11 | ZC98 | 0 | Amorphous | - | - | - | - | - | - |
| | ZC99 | 3 | Amorphous | - | - | - | - | - | - |
| | ZC100 | 6 | Amorphous Major ZSM-35 Minor | 28.22 | 2.65 | 9.39 | 0.32 | 0.80 | 25.6 |
| | ZC101 | 10 | ZSM-35 | 26.44 | 2.33 | 8.81 | 1.00 | 0.75 | 75 |
| | ZC67 | 15 | ZSM-35 Major Mordenite Minor | 28.02 | 2.34 | 8.35 | 1.00 | 0.71 | 71 |
| | ZC68 | 24 | ZSM-35 Major Mordenite minor | 28.18 | 2.48 | 8.80 | 1.02 | 0.75 | 76.5 |

*Table A.8 Crystallization of ZSM-35 from a Molar Batch Composition of 1.85 $Na_2O$. $Al_2O_3$. 20 $SiO_2$. 592 $H_2O$. 19.7 ED at T = 225 °C*

| Batch Code | Sample Code | Crystallization Time (h) | Crystalline Phases | Weight of Batch (g) | Weight of Product (g) | % Yield | Crystallinity Index | Yield/ Maximum Yield | % Conversion |
|---|---|---|---|---|---|---|---|---|---|
| Z15 | ZC102 | 0 | Amorphous | - | - | - | - | - | - |
| | ZC103 | 5 | ZSM-35 Major Amorphous Minor | 23.07 | 2.08 | 9.02 | 0.59 | 0.75 | 44.3 |
| | ZC1104 | 8 | ZSM-35 | 29.32 | 2.89 | 9.86 | 0.83 | 0.82 | 68 |
| | ZC105 | 12 | ZSM-35 | 28.16 | 2.55 | 9.06 | 0.89 | 0.76 | 67.6 |
| | ZC85 | 15 | ZSM-35 | 29.74 | 2.37 | 7.97 | 0.94 | 0.67 | 63 |
| | ZC86 | 24 | ZSM-35 | 29.44 | 2.45 | 8.32 | 1.02 | 0.70 | 71 |

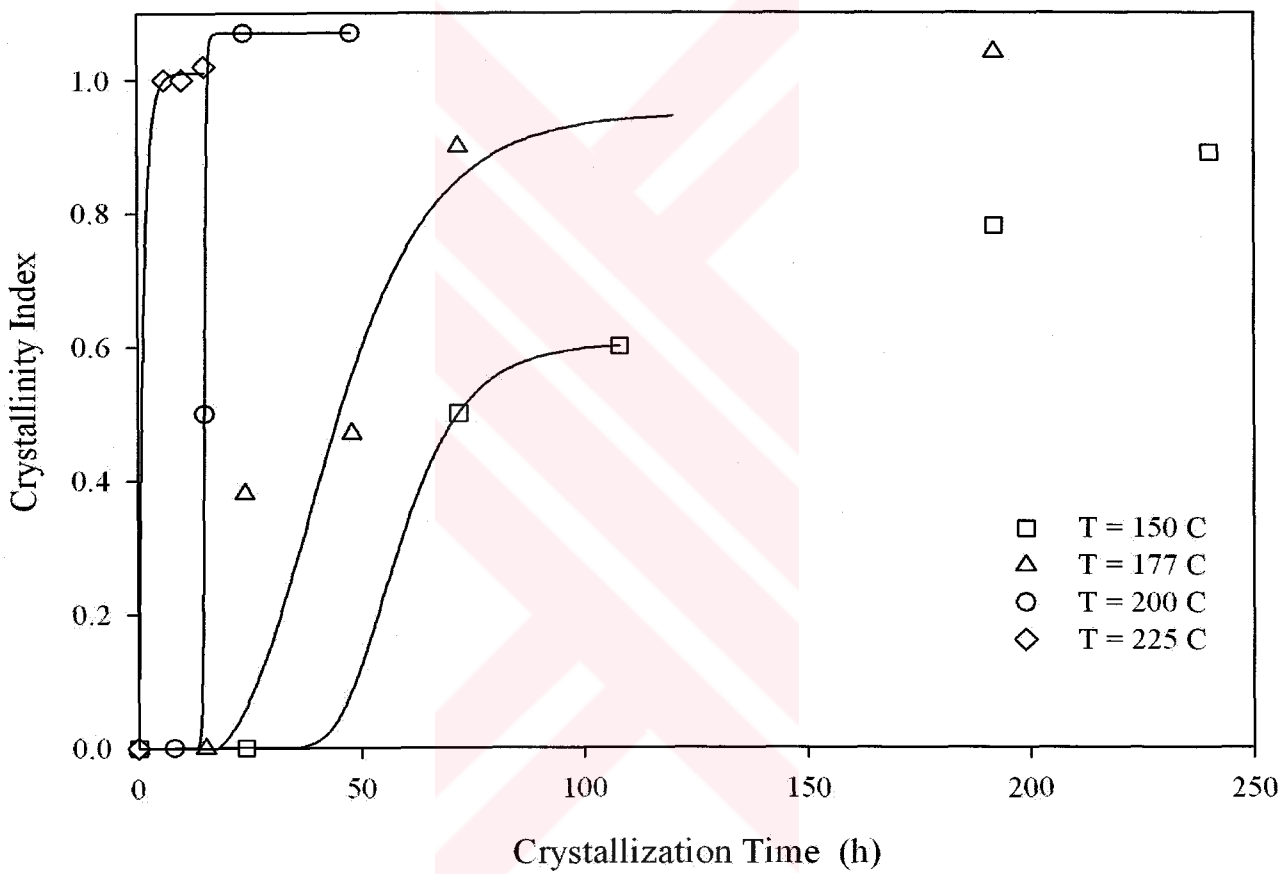


*Figure A.1 Effect of Temperature on Crystallization of ZSM-35 from a Molar Batch Composition of 1.85 $Na_2O$. $Al_2O_3$. 20 $SiO_2$. 592 $H_2O$. 19.7 Py*

# APPENDIX B

# CHARACTERIZATION

## B.1 X-Ray Diffraction Patterns

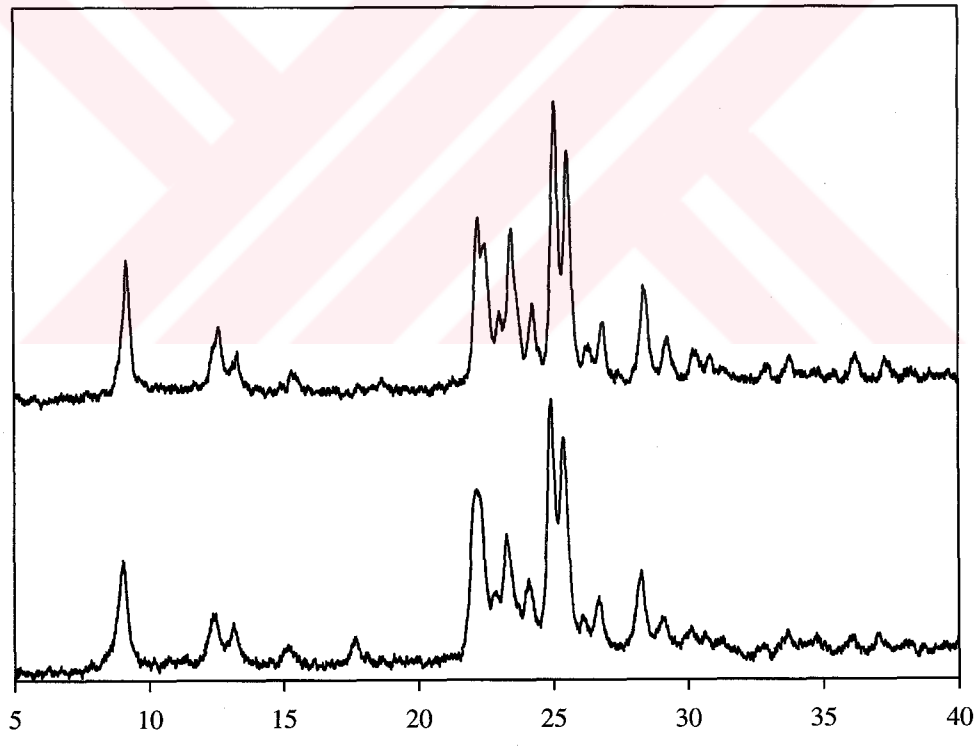


*Figure B.1 Comparison of XRD Patterns of Samples Synthesized with Pyrrolidine (Bottom) and Ethylenediamine (Top) at the $SiO_2/Al_2O_3$ ratio of 20 at 150 °C*

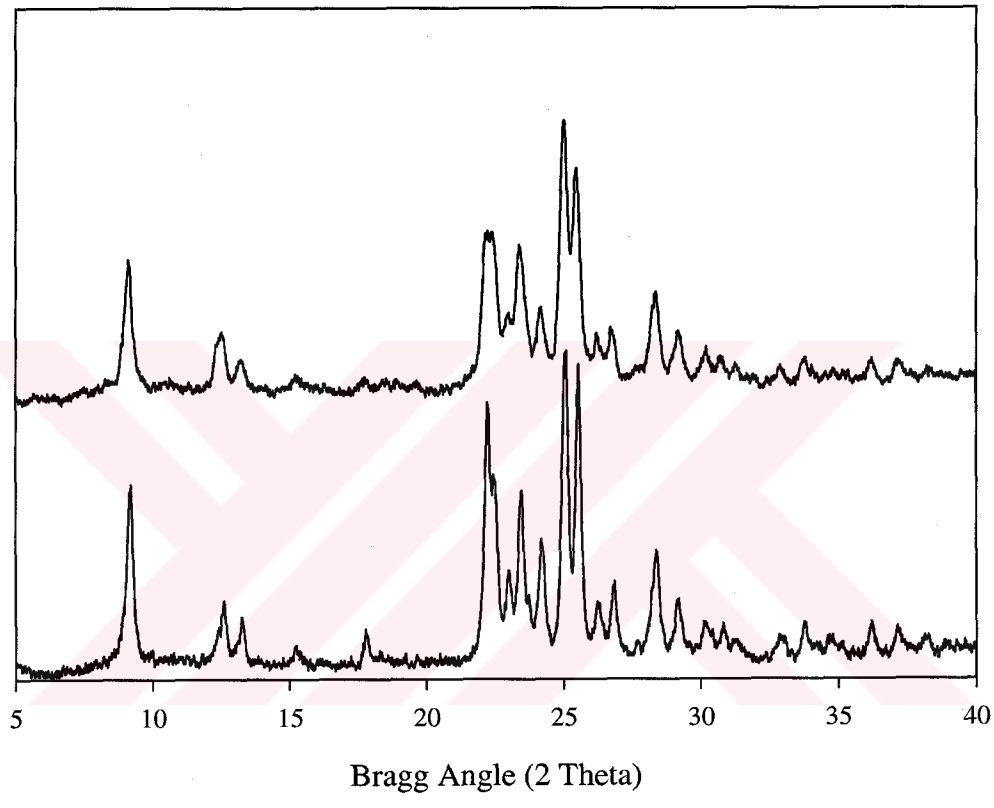


*Figure B.2 Comparison of XRD Patterns of Samples Synthesized with Pyrrolidine (Bottom) and Ethylenediamine (Top) at the $SiO_2/Al_2O_3$ Ratio of 20 at 177 °C*

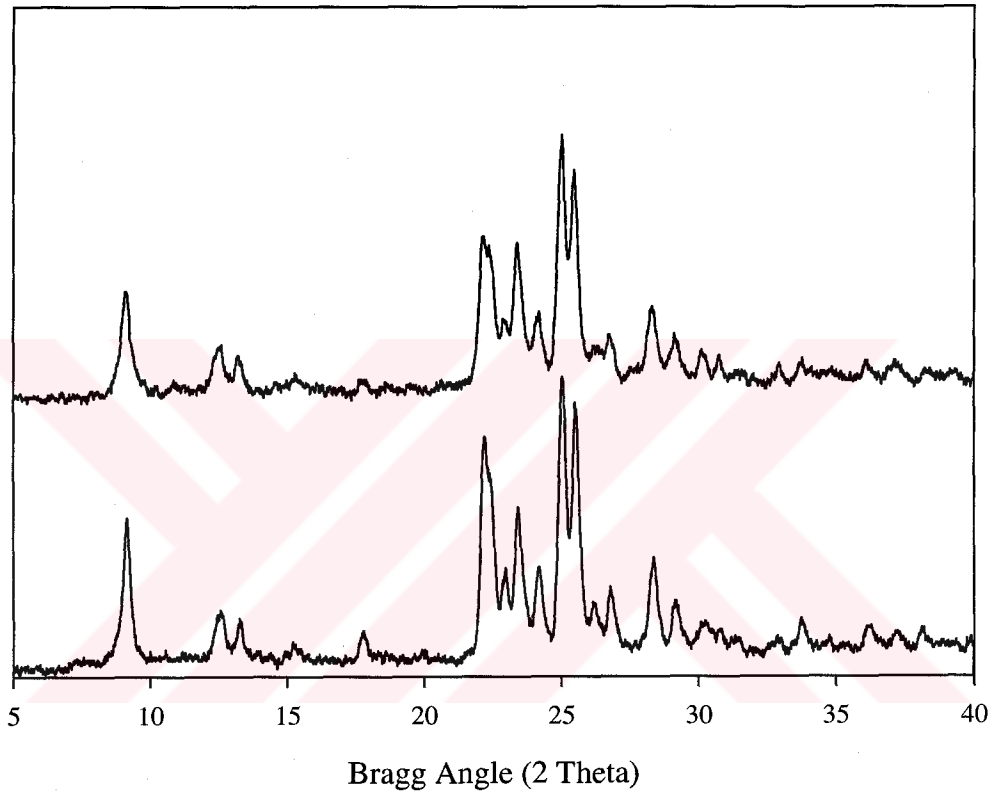


*Figure B.3 Comparison of XRD Patterns of Samples Synthesized with Pyrrolidine (Bottom) and Ethylenediamine (Top) at the $SiO_2/Al_2O_3$ Ratio of 20 at 200 °C*

## B.2 Scanning Electron Micrographs

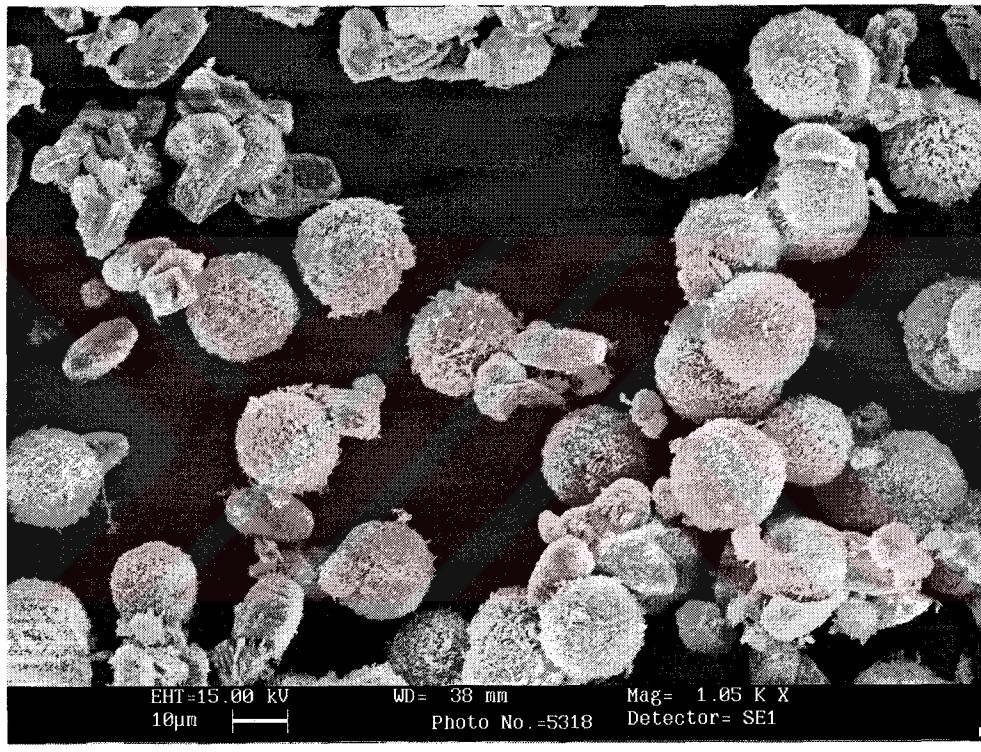


*Figure B.4 SEM Micrograph of Sample ZC42 (Batch Code Z5, Part 1) Synthesized at 177 °C for 8 Days with Template Pyrrolidine.*

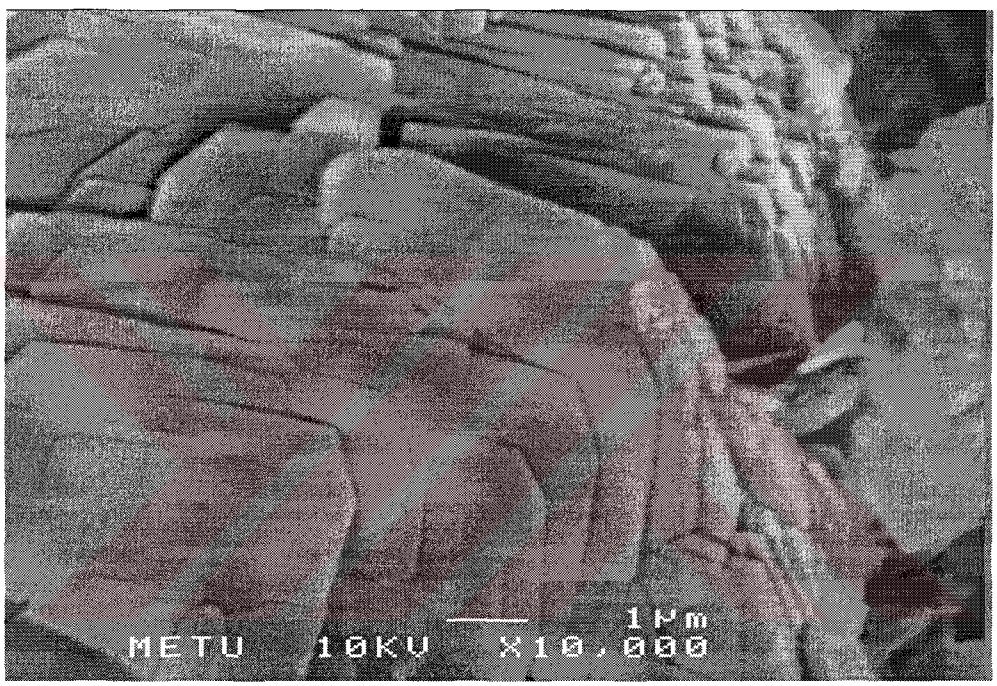


*Figure B.5 SEM Micrograph of Sample ZC86 (Batch Code Z15, Part 3) Synthesized at 225 °C for 1 Days with Template Ethylenediamine.*

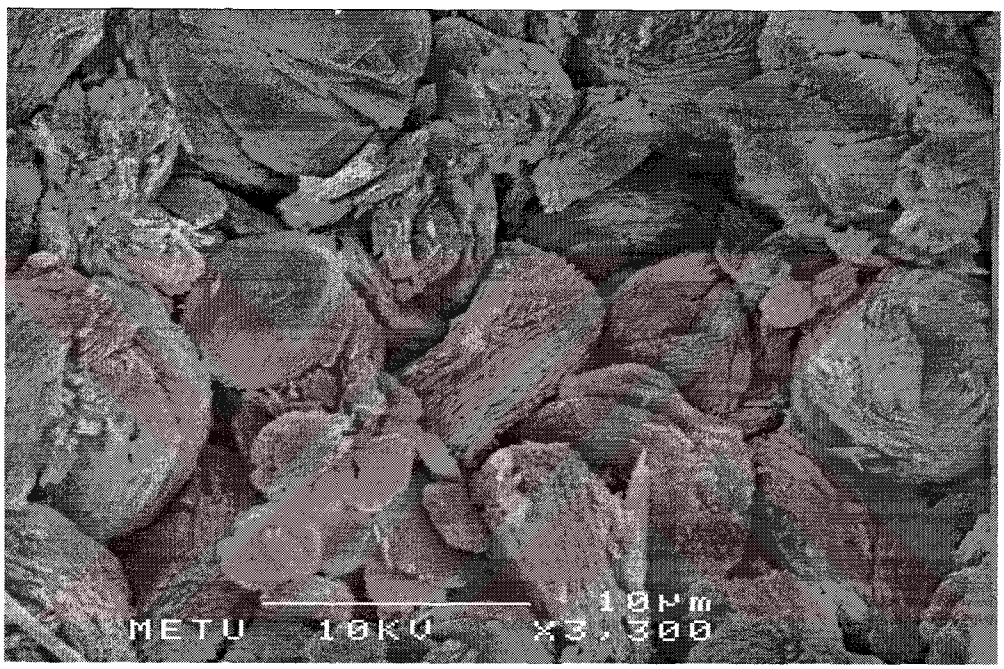


*Figure B.6 SEM Micrograph of Sample ZC83 (Batch Code Z14, Part 3) Synthesized at 200 °C for 5 Days with Template Ethylenediamine.*

# APPENDIX C

# X-RAY DIFFRACTION DATA

*Table C.1 Peak Listing of Natural Ferrierite from Kamloops Given by Kibby et al. (1974)*

| Peak No | d-Spacing | Bragg Angle 2 (Theta) | $I/I_0$ |
|---|---|---|---|
| | 11.3 | 7.82 | 20 |
| 1 | 9.61 | 9.2 | 100 |
| 2 | 7.00 | 12.65 | 30 |
| 3 | 6.61 | 13.42 | 20 |
| 4 | 5.84 | 15.17 | 50 |
| | 3.99 | 22.28 | 90 |
| 7 | 3.88 | 22.92 | 10 |
| 9 | 3.79 | 23.47 | 20 |
| | 3.69 | 24.12 | 50 |
| 11 | 3.54 | 25.16 | 80 |
| 12 | 3.49 | 25.52 | 80 |
| 14 | 3.31 | 26.94 | 20 |
| 15 | 3.15 | 28.33 | 30 |
| | 3.07 | 29.09 | 30 |
| | 2.97 | 30.09 | 30 |
| | 2.90 | 30.83 | 20 |
| | 2.58 | 34.77 | 30 |

*Table C.2 Peak Listing of Natural Ferrierite from Aqoura Given by Kibby et al. (1974)*

| Peak No | d-Spacing | Bragg Angle 2 (Theta) | $I/I_0$ |
|---|---|---|---|
| | 11.3 | 7.82 | 3 |
| 1 | 9.47 | 9.34 | 50 |
| 2 | 7.07 | 12.52 | 38 |
| 3 | 6.59 | 13.44 | 3 |
| 4 | 5.75 | 15.41 | 15 |
| | 5.64 | 15.71 | 14 |
| 6 | 3.98 | 22.34 | 35 |
| 7 | 3.94 | 22.57 | 35 |
| 9 | 3.78 | 23.54 | 65 |
| 10 | 3.66 | 24.32 | 12 |
| | 3.54 | 25.16 | 100 |
| 12 | 3.48 | 25.6 | 18 |
| 14 | 3.31 | 26.94 | 35 |
| 15 | 3.14 | 28.42 | 12 |
| 16 | 3.05 | 29.28 | 12 |

*Table C.3 Peak Listing of Natural Ferrierite from Sonora Pass Given by Kibby et al. (1974)*

| Peak No | d-Spacing | Bragg Angle 2 (Theta) | $I/I_0$ |
|---|---|---|---|
| 1 | 9.56 | 9.25 | 80 |
| 2 | 7.06 | 12.54 | 12 |
| 3 | 6.61 | 13.39 | 8 |
| 4 | 5.83 | 15.2 | 21 |
| | 5.71 | 15.52 | 8 |
| 6 | 3.99 | 22.28 | 29 |
| | 3.97 | 22.39 | 60 |
| | 3.79 | 23.47 | 55 |
| | 3.70 | 24.05 | 37 |
| 11 | 3.53 | 25.23 | 100 |
| 12 | 3.49 | 25.52 | 50 |
| 14 | 3.32 | 26.85 | 13 |
| | 3.15 | 28.33 | 9 |
| | 3.07 | 29.09 | 13 |
| | 2.98 | 29.98 | 22 |

*Table C.4 Peak Listing of Natural Ferrierite Given by Vaughan (1966)*

| Peak No | d-Spacing | Bragg Angle 2 (Theta) | $I/I_0$ | Peak No | d-Spacing | Bragg Angle 2 (Theta) | $I/I_0$ |
|---|---|---|---|---|---|---|---|
| | 11.36 | 7.78 | 58.80 | 19 | 2.64 | 33.91 | 4.20 |
| 1 | 9.58 | 9.23 | 100.00 | | 2.63 | 34.08 | 0.70 |
| 2 | 7.06 | 12.53 | 9.20 | | 2.58 | 34.72 | 2.80 |
| | 6.98 | 12.69 | 13.70 | | 2.57 | 34.91 | 0.70 |
| 3 | 6.62 | 13.38 | 7.90 | | 2.57 | 34.92 | 1.10 |
| | 5.82 | 15.23 | 26.10 | | 2.49 | 36.04 | 0.80 |
| | 5.68 | 15.59 | 2.50 | | 2.48 | 36.20 | 1.30 |
| | 5.44 | 16.28 | 0.20 | 20 | 2.48 | 36.29 | 0.20 |
| 5 | 4.96 | 17.87 | 5.50 | | 2.43 | 37.00 | 2.80 |
| | 4.86 | 18.26 | 0.50 | | 2.42 | 37.22 | 0.60 |
| | 4.79 | 18.53 | 2.20 | | 2.39 | 37.56 | 0.20 |
| | 4.57 | 19.41 | 1.80 | | 2.37 | 37.99 | 0.20 |
| | 4.00 | 22.21 | 26.20 | | 2.37 | 38.03 | 3.30 |
| 6 | 3.99 | 22.30 | 7.70 | | 2.34 | 38.54 | 0.60 |
| | 3.96 | 22.43 | 21.10 | | 2.32 | 38.73 | 0.20 |
| | 3.88 | 22.92 | 15.00 | | 2.31 | 38.91 | 2.20 |
| 9 | 3.79 | 23.47 | 16.80 | | 2.30 | 39.21 | 0.40 |
| | 3.74 | 23.76 | 3.60 | | 2.29 | 39.41 | 0.20 |
| | 3.70 | 24.07 | 6.70 | | 2.27 | 39.63 | 0.20 |
| | 3.56 | 25.04 | 15.70 | | 2.27 | 39.75 | 0.30 |
| 11 | 3.53 | 25.22 | 29.20 | | 2.26 | 39.81 | 1.10 |
| 12 | 3.49 | 25.54 | 35.60 | | | | |
| | 3.41 | 26.13 | 6.10 | | | | |
| | 3.31 | 26.91 | 6.80 | | | | |
| 14 | 3.31 | 26.95 | 0.60 | | | | |
| | 3.19 | 27.95 | 1.20 | | | | |
| | 3.15 | 28.32 | 1.60 | | | | |
| | 3.15 | 28.34 | 13.58 | | | | |
| 15 | 3.13 | 28.54 | 1.80 | | | | |
| | 3.07 | 29.07 | 9.20 | | | | |
| | 3.06 | 29.15 | 0.10 | | | | |
| | 2.97 | 30.07 | 7.60 | | | | |
| 17 | 2.95 | 30.30 | 2.30 | | | | |
| 18 | 2.91 | 30.73 | 0.20 | | | | |
| | 2.90 | 30.86 | 5.10 | | | | |
| | 2.88 | 31.10 | 0.80 | | | | |
| | 2.86 | 31.31 | 0.20 | | | | |
| | 2.84 | 31.47 | 0.80 | | | | |
| | 2.80 | 32.02 | 0.40 | | | | |
| | 2.72 | 32.90 | 3.60 | | | | |
| | 2.69 | 33.35 | 0.90 | | | | |

*Table C.5 Peak Listing of Natural Ferrierite of PDF # 39-1382*

| Peak No | d-Spacing | Bragg Angle 2 (Theta) | $I/I_0$ |
|---|---|---|---|
| | 11.38 | 7.76 | 3 |
| 1 | 9.60 | 9.20 | 100 |
| 2 | 6.98 | 12.67 | 5 |
| 3 | 6.63 | 13.34 | 3 |
| | 5.84 | 15.16 | 18 |
| 5 | 4.97 | 17.83 | 2 |
| | 4.80 | 18.47 | 5 |
| | 4.58 | 19.37 | 2 |
| | 4.01 | 22.15 | 21 |
| 6 | 3.97 | 22.35 | 38 |
| 7 | 3.88 | 22.85 | 14 |
| | 3.79 | 23.41 | 20 |
| | 3.71 | 23.98 | 31 |
| | 3.56 | 24.98 | 14 |
| 11 | 3.53 | 25.17 | 26 |
| 12 | 3.49 | 25.48 | 22 |
| | 3.42 | 26.06 | 8 |
| | 3.32 | 26.85 | 7 |
| 14 | 3.31 | 26.91 | 6 |
| | 3.19 | 27.87 | 9 |
| | 3.15 | 28.3 | 10 |
| 15 | 3.13 | 28.49 | 4 |
| | 3.07 | 29 | 12 |
| | 2.97 | 29.99 | 13 |
| 17 | 2.95 | 30.22 | 4 |
| | 2.90 | 30.79 | 4 |
| | 2.84 | 31.41 | 1 |
| | 2.72 | 32.83 | 5 |
| | 2.69 | 33.20 | 6 |
| | 2.64 | 33.89 | 3 |
| | 2.58 | 34.73 | 4 |
| | 2.57 | 34.85 | 3 |
| | 2.43 | 36.93 | 4 |
| | 2.37 | 37.9 | 9 |
| | 2.32 | 38.8 | 1 |
| | 2.25 | 39.94 | 2 |

*Table C.6 Peak Listing of Synthetic Ferrierite Given by Barrer and Marshall (1965)*

| Peak No | d-Spacing | Bragg Angle 2 (Theta) | $I/I_0$ |
|---|---|---|---|
| 1 | 9.49 | 9.32 | 75 |
| 2 | 7.07 | 12.52 | 20 |
| 3 | 6.61 | 13.39 | 55 |
| 4 | 5.77 | 15.36 | 15 |
| 6 | 3.99 | 22.28 | 45 |
| 7 | 3.94 | 22.57 | 35 |
| | 3.86 | 23.04 | 25 |
| 9 | 3.78 | 23.54 | 50 |
| | 3.67 | 24.25 | 30 |
| 11 | 3.54 | 25.16 | 90 |
| 12 | 3.48 | 25.6 | 100 |
| 14 | 3.31 | 26.94 | 20 |
| 15 | 3.14 | 28.42 | 55 |
| | 3.06 | 29.18 | 45 |
| 17 | 2.96 | 30.19 | 25 |
| | 2.90 | 30.83 | 35 |
| | 2.58 | 34.77 | 10 |

*Table C.7 Peak Listing of Synthetic Ferrierite of Hawkins Given by Kibby et al. (1974)*

| Peak No | d-Spacing | Bragg Angle 2 (Theta) | $I/I_0$ |
|---|---|---|---|
| 1 | 9.45 | 9.36 | 40 |
| 2 | 7.02 | 12.61 | 10 |
| 3 | 6.58 | 13.46 | 30 |
| 4 | 5.77 | 15.36 | 10 |
| 6 | 3.97 | 22.39 | 50 |
| 7 | 3.94 | 22.57 | 40 |
| 8 | 3.86 | 23.04 | 40 |
| 9 | 3.78 | 23.54 | 50 |
| 10 | 3.66 | 24.32 | 30 |
| 11 | 3.52 | 25.3 | 100 |
| 12 | 3.47 | 25.67 | 80 |
| 14 | 3.31 | 26.94 | 20 |
| 15 | 3.14 | 28.42 | 50 |
| 16 | 3.05 | 29.28 | 40 |
| 17 | 2.95 | 30.3 | 30 |
| | 2.89 | 30.94 | 40 |
| | 2.60 | 34.5 | 10 |

*Table C.8 Peak Listing of Synthetic Ferrierite of Senderov Given by Kibby et al. (1974)*

| Peak No | d-Spacing | Bragg Angle 2 (Theta) | $I/I_0$ |
|---|---|---|---|
| 1 | 9.57 | 9.24 | 100 |
| 2 | 7.12 | 12.43 | 20 |
| 3 | 6.70 | 13.21 | 20 |
| 4 | 5.68 | 15.6 | 40 |
| 6 | 4.00 | 22.22 | 80 |
| 9 | 3.76 | 23.66 | 60 |
| 10 | 3.66 | 24.32 | 40 |
| | 3.57 | 24.94 | 50 |
| 12 | 3.49 | 25.52 | 70 |
| | 3.33 | 26.77 | 10 |
| | 3.15 | 28.33 | 40 |
| | 3.06 | 29.18 | 20 |
| | 2.91 | 30.72 | 10 |
| | 2.57 | 34.91 | 10 |

*Table C.9 Peak Listing of Synthetic Ferrierite Given by Kibby et al.(1974)*

| Peak No | d-Spacing | Bragg Angle 2 (Theta) | $I/I_0$ |
|---|---|---|---|
| 1 | 9.41 | 9.4 | 100 |
| 2 | 7.00 | 12.65 | 24 |
| 3 | 6.56 | 13.5 | 24 |
| 4 | 5.72 | 15.49 | 12 |
| | 5.61 | 15.8 | 12 |
| 6 | 3.97 | 22.39 | 45 |
| 7 | 3.92 | 22.68 | 37 |
| 8 | 3.83 | 23.22 | 27 |
| | 3.75 | 23.73 | 40 |
| 10 | 3.65 | 24.39 | 34 |
| 11 | 3.52 | 25.3 | 65 |
| 12 | 3.47 | 25.67 | 58 |
| 14 | 3.30 | 27.02 | 15 |
| | 3.15 | 28.33 | 28 |
| 16 | 3.04 | 29.38 | 20 |
| | 2.94 | 30.4 | 10 |
| | 2.88 | 31.05 | 10 |
| | 2.56 | 35.05 | 3 |

*Table C.10 Peak Listing of Synthetic Ferrierite Given by Plank et al. (1977)*

| Peak No | d-Spacing | Bragg Angle 2 (Theta) | $I/I_0$ |
|---|---|---|---|
| | 11.33 | 7.80 | 1 |
| 1 | 9.59 | 9.22 | 124 |
| 2 | 7.08 | 12.50 | 26 |
| | 6.98 | 12.68 | 38 |
| 3 | 6.63 | 13.35 | 22 |
| | 6.44 | 13.75 | 1 |
| 4 | 5.78 | 15.34 | 10 |
| | 5.68 | 15.60 | 6 |
| 5 | 4.97 | 17.85 | 6 |
| | 4.83 | 18.35 | 1 |
| | 4.74 | 18.72 | 3 |
| | 4.57 | 19.42 | 1 |
| 5 | 3.99 | 22.29 | 77 |
| 7 | 3.93 | 22.60 | 50 |
| 8 | 3.85 | 23.12 | 28 |
| 9 | 3.78 | 23.55 | 55 |
| | 3.74 | 23.80 | 6 |
| 10 | 3.66 | 24.32 | 33 |
| 11 | 3.54 | 25.14 | 100 |
| 12 | 3.48 | 25.61 | 83 |
| 13 | 3.38 | 26.39 | 15 |
| 14 | 3.31 | 26.92 | 17 |
| 15 | 3.14 | 28.45 | 15 |
| 16 | 3.05 | 29.30 | 17 |
| 17 | 2.95 | 30.30 | 8 |
| | 2.89 | 30.90 | 7 |
| | 2.84 | 31.50 | 3 |
| | 2.71 | 33.09 | 4 |
| 19 | 2.65 | 33.88 | 7 |
| | 2.61 | 34.37 | 2 |
| | 2.58 | 34.79 | 3 |
| | 2.54 | 35.30 | 2 |
| 20 | 2.48 | 36.29 | 6 |
| | 2.45 | 36.70 | 1 |
| | 2.41 | 37.35 | 4 |
| | 2.39 | 37.65 | 1 |

*Table C.11 Peak Listing of Synthetic Ferrierite Given by Çulfaz and Yılmaz (1985)*

| Peak No | d-Spacing | Bragg Angle 2 (Theta) | $I/I_0$ |
|---|---|---|---|
| | 9.38 | 9.43 | 86 |
| 2 | 7.05 | 12.56 | 48 |
| | 6.90 | 12.83 | 35 |
| | 6.51 | 13.6 | 25 |
| 4 | 5.73 | 15.46 | 24 |
| | 5.65 | 15.68 | 31 |
| 6 | 3.98 | 22.34 | 45 |
| 7 | 3.90 | 22.8 | 33 |
| | 3.83 | 23.22 | 26 |
| 9 | 3.77 | 23.6 | 55 |
| | 3.64 | 24.45 | 27 |
| 11 | 3.53 | 25.23 | 100 |
| 12 | 3.46 | 25.75 | 71 |
| 14 | 3.32 | 26.85 | 29 |
| 15 | 3.12 | 28.61 | 36 |
| 16 | 3.04 | 29.38 | 28 |
| | 2.89 | 30.94 | 12 |
| | 2.70 | 33.18 | 11 |

*Table C.12 Peak Listing of Synthetic Ferrierite Given by Wenyang et al. (1989)*

| Peak No | d-Spacing | Bragg Angle 2 (Theta) | $I/I_0$ |
|---|---|---|---|
| 1 | 9.51 | 9.30 | 129 |
| 2 | 7.1 | 12.47 | 28 |
| | 6.99 | 12.66 | 22 |
| 3 | 6.66 | 13.29 | 16 |
| 4 | 5.79 | 15.30 | 10 |
| | 5.68 | 15.60 | 8 |
| 5 | 4.98 | 17.81 | 4 |
| | 4.52 | 19.64 | 10 |
| 6 | 4 | 22.22 | 59 |
| 7 | 3.95 | 22.51 | 44 |
| | 3.87 | 22.98 | 37 |
| | 3.79 | 23.47 | 72 |
| | 3.75 | 23.73 | 23 |
| 10 | 3.66 | 24.32 | 33 |
| 11 | 3.53 | 25.23 | 100 |
| 12 | 3.47 | 25.67 | 80 |
| 13 | 3.39 | 26.29 | 28 |
| 14 | 3.31 | 26.94 | 24 |
| 15 | 3.13 | 28.52 | 18 |
| 17 | 2.95 | 30.30 | 6 |
| | 2.91 | 30.72 | 2 |
| | 2.7 | 33.18 | 3 |

*Table C.13 Peak Listing of Synthetic Ferrierite Given by Borade and Clearfield (1994)*

| Peak No | d-Spacing | Bragg Angle (2 Theta) | I/Io |
|---|---|---|---|
| 1 | 9.5 | 9.31 | 78 |
| 2 | 7.03 | 12.59 | 21 |
| | 6.97 | 12.70 | 24 |
| 3 | 6.6 | 13.42 | 26 |
| 4 | 5.77 | 15.36 | 13 |
| | 5.67 | 15.63 | 12 |
| 5 | 4.96 | 17.88 | 22 |
| 6 | 3.98 | 22.34 | 54 |
| 7 | 3.94 | 22.57 | 39 |
| 8 | 3.85 | 23.10 | 50 |
| 9 | 3.77 | 23.60 | 30 |
| 10 | 3.66 | 24.32 | 33 |
| 11 | 3.53 | 25.23 | 100 |
| 12 | 3.48 | 25.60 | 68 |
| 13 | 3.38 | 26.37 | 19 |
| 14 | 3.31 | 26.94 | 22 |
| 15 | 3.14 | 28.42 | 26 |
| 16 | 3.05 | 29.28 | 13 |
| 18 | 2.89 | 30.94 | 11 |

*Table C.14 Peak Listing of Synthetic Ferrierite Given by Robson (1998)*

| Peak No | d-Spacing | Bragg Angle (2 Theta) | I/Io |
|---|---|---|---|
| 1 | 9.53 | 9.28 | 36 |
| 2 | 7.07 | 12.52 | 8 |
| 3 | 6.61 | 13.39 | 17 |
| 4 | 5.76 | 15.38 | 8 |
| 5 | 4.95 | 17.92 | 8 |
| | 4.48 | 19.8 | 4 |
| 6 | 3.98 | 22.34 | 65 |
| 7 | 3.93 | 22.62 | 43 |
| 8 | 3.85 | 23.1 | 29 |
| 9 | 3.77 | 23.6 | 52 |
| 10 | 3.66 | 24.32 | 29 |
| 11 | 3.53 | 25.23 | 100 |
| 12 | 3.47 | 25.67 | 98 |
| 13 | 3.39 | 26.29 | 17 |
| 14 | 3.31 | 26.94 | 17 |
| 15 | 3.13 | 28.52 | 32 |
| 16 | 3.04 | 29.38 | 14 |
| 17 | 2.95 | 30.26 | 10 |
| 18 | 2.92 | 30.65 | 14 |
| | 2.71 | 33 | 4 |
| 19 | 2.64 | 33.98 | 9 |
| | 2.57 | 34.9 | 3 |
| 20 | 2.47 | 36.33 | 12 |
| | 2.43 | 37 | 6 |

*Table C.15 Peak Listing of Synthetic Ferrierite Given by Tütüncü (2003)*

| Peak No | d-Spacing | Bragg Angle (2 Theta) | I/Io |
|---|---|---|---|
| 1 | 9.53 | 9.28 | 54 |
| | 9.17 | 9.65 | 9 |
| 2 | 7.07 | 12.52 | 11 |
| | 6.93 | 12.77 | 14 |
| 3 | 6.61 | 13.39 | 18 |
| 4 | 5.76 | 15.38 | 12 |
| | 4.72 | 18.80 | 15 |
| 6 | 3.98 | 22.34 | 43 |
| 7 | 3.93 | 22.62 | 12 |
| 8 | 3.85 | 23.10 | 15 |
| 9 | 3.77 | 23.60 | 54 |
| | 3.74 | 23.8 | 5 |
| 10 | 3.66 | 24.32 | 41 |
| 11 | 3.53 | 25.23 | 100 |
| 12 | 3.47 | 25.67 | 75 |
| | 3.42 | 26.08 | 18 |
| 14 | 3.31 | 26.94 | 23 |
| 15 | 3.13 | 28.52 | 30 |
| 16 | 3.04 | 29.38 | 18 |
| 18 | 2.92 | 30.65 | 8 |
| 19 | 2.64 | 33.98 | 12 |
| 20 | 2.47 | 36.35 | 11 |
| | 2.35 | 38.33 | 9 |

*Table C.16 Peak Listing of Synthetic Ferrierite Synthesized in This Study (ZC42)*

| Peak No | d-Spacing | Bragg Angle (2 Theta) | I/Io |
|---|---|---|---|
| 1 | 9.61 | 9.2 | 57.45 |
| 2 | 7.08 | 12.5 | 20.43 |
| 3 | 6.71 | 13.2 | 14.89 |
| 4 | 5.83 | 15.2 | 6.38 |
| 5 | 4.98 | 17.8 | 11.49 |
| 6 | 4.00 | 22.2 | 82.98 |
| 7 | 3.95 | 22.5 | 59.57 |
| 8 | 3.87 | 23.0 | 31.91 |
| 9 | 3.79 | 23.5 | 57.45 |
| 10 | 3.68 | 24.2 | 39.15 |
| 11 | 3.55 | 25.1 | 100 |
| 12 | 3.49 | 25.5 | 94.47 |
| 13 | 3.40 | 26.2 | 19.15 |
| 14 | 3.33 | 26.8 | 25.53 |
| 15 | 3.14 | 28.4 | 36.17 |
| 16 | 3.07 | 29.1 | 21.28 |
| 17 | 2.97 | 30.1 | 12.77 |
| 18 | 2.90 | 30.8 | 12.77 |
| 19 | 2.65 | 33.8 | 12.77 |
| 20 | 2.48 | 36.2 | 12.77 |